



HAL
open science

Satellite altimeter-derived monthly discharge of the Ganga-Brahmaputra River and its seasonal to interannual variations from 1993 to 2008

Fabrice Papa, Fabien Durand, William B. Rossow, Altiquir Rahman, Sujit Bala

► **To cite this version:**

Fabrice Papa, Fabien Durand, William B. Rossow, Altiquir Rahman, Sujit Bala. Satellite altimeter-derived monthly discharge of the Ganga-Brahmaputra River and its seasonal to interannual variations from 1993 to 2008. *Journal of Geophysical Research*, 2010, 115 (C12), pp.C12013. 10.1029/2009JC006075 . hal-00798718

HAL Id: hal-00798718

<https://hal.science/hal-00798718>

Submitted on 5 Jun 2014

HAL is a multi-disciplinary open access archive for the deposit and dissemination of scientific research documents, whether they are published or not. The documents may come from teaching and research institutions in France or abroad, or from public or private research centers.

L'archive ouverte pluridisciplinaire **HAL**, est destinée au dépôt et à la diffusion de documents scientifiques de niveau recherche, publiés ou non, émanant des établissements d'enseignement et de recherche français ou étrangers, des laboratoires publics ou privés.

Satellite altimeter-derived monthly discharge of the Ganga-Brahmaputra River and its seasonal to interannual variations from 1993 to 2008

Fabrice Papa,^{1,2} Fabien Durand,³ William B. Rossow,¹ Atiqur Rahman,¹ and Sujit K. Bala⁴

Received 21 December 2009; revised 6 August 2010; accepted 18 August 2010; published 4 December 2010.

[1] The Ganga-Brahmaputra accounts for ~25% of the total amount of freshwater received by the Bay of Bengal. Using daily in situ river discharge data along with altimetry-derived river heights, the present study aims to produce a monthly data set of altimetry-derived Ganga-Brahmaputra River discharge at the river mouths for 1993–2008. First, we estimate the standard error of ENVISAT-derived water levels over the Ganga to be 0.26 m, much smaller than the range of variability of ~7 m, and consistent with the accuracy of altimeter measurements over large rivers. We then establish rating curves between altimetry-derived water levels and in situ river discharges and show that TOPEX-Poseidon, ERS-2, and ENVISAT data can successfully be used to infer Ganga and Brahmaputra discharge. The mean error on the estimated daily discharge derived from altimetry ranges from ~15% (~4700 m³/s) using TOPEX-Poseidon over the Brahmaputra to ~36% (~9000 m³/s) using ERS-2 over the Ganga. Combined Ganga-Brahmaputra monthly discharges for 1993–2008 are presented, showing a mean error of ~17% (~2700 m³/s), within the range (15%–20%) of acceptable accuracy for discharge measurements. During 2004–2008, we assess the variability of the estimate against precipitation and river heights records. Finally, we present a basic approach to infer Ganga-Brahmaputra monthly discharge at the river mouths. The upscaled discharge exhibits a marked interannual variability with a standard deviation in excess of ~12,500 m³/s, much larger than the data set uncertainty. This new data set represents an unprecedented source of information to quantify continental freshwater forcing flux into Indian Ocean circulation models.

Citation: Papa, F., F. Durand, W. B. Rossow, A. Rahman, and S. K. Bala (2010), Satellite altimeter-derived monthly discharge of the Ganga-Brahmaputra River and its seasonal to interannual variations from 1993 to 2008, *J. Geophys. Res.*, 115, C12013, doi:10.1029/2009JC006075.

1. Introduction

[2] The Bay of Bengal (BoB, Figure 1a) in the northern Indian Ocean plays a key role in the tropical climate system. It is hypothesized that the intensity of air-sea coupling in this area has a strong impact on the Asian monsoon as well as on the cyclonic activity in the region [Sengupta *et al.*, 2008; McPhaden *et al.*, 2009]. Compared to the rest of the Indo-Pacific warm pool, the Bay of Bengal is characterized by a strong ocean salinity stratification resulting from an excess of freshwater supply over evaporation [Vinayachandran *et al.*, 2002]. The Bay of Bengal is indeed subject to strong precipitation [Hoyos and Webster, 2007] and receives a large

amount of freshwater from the surrounding continents via river discharge [Shetye, 1993; Sengupta *et al.*, 2006]. Because of the smaller density of freshwater compared to salty water, the sharp salinity stratification stabilizes the water column which prevents mixing with the underlying cooler thermocline waters and enhances the heating of the surface waters [Schott *et al.*, 2009]. This results in very high sea surface temperatures (SSTs; typically above 28°C) throughout the Bay of Bengal in all seasons, favoring monsoonal convective activity primarily locked to the bay and the surrounding continent, which in turn generates intense continental and atmospheric freshwater supply to the ocean. This positive feedback cycle characterizes the climate of the area [Shenoi *et al.*, 2002].

[3] If the spatiotemporal distribution of precipitation over the BoB are nowadays well documented [Xie and Arkin, 1997; Adler *et al.*, 2003; Hoyos and Webster, 2007; Rahman *et al.*, 2009], much less is known about the contribution of continental runoff from surrounding rivers and its impact on ocean salinity and temperature variability and oceanic circulation. It is suggested that continental discharge accounts for about

¹NOAA-CREST, City College of New York, New York, New York, USA.

²Now at IRD-LEGOS, Toulouse, France.

³IRD-LEGOS, Nouméa, New Caledonia.

⁴Institute of Water and Flood Management, Bangladesh University of Engineering and Technology, Dhaka, Bangladesh.

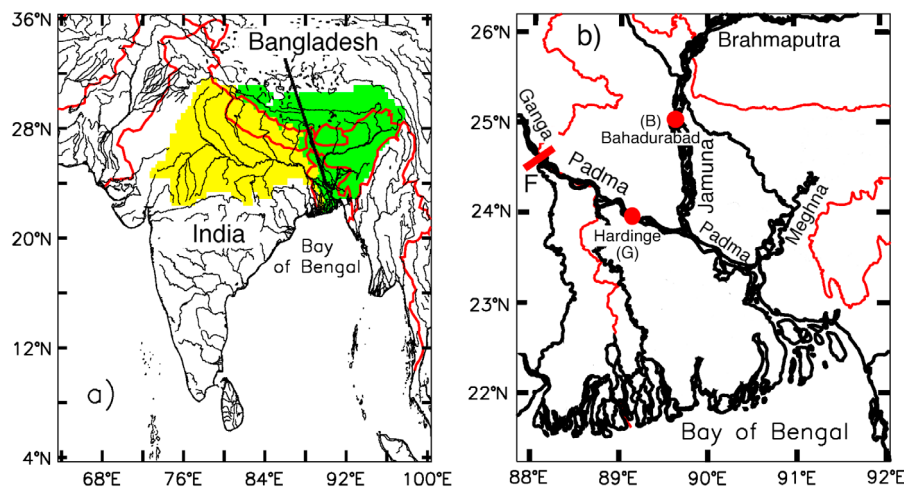


Figure 1. The Ganga and Brahmaputra systems, which flow into the Bay of Bengal. (a) The region of interest with the catchments areas of the Ganga (yellow) and the Brahmaputra (green) rivers. The red lines show the political borders. (b) Detailed map with the locations of the two gauging stations in Bangladesh, Hardinge (G) and Bahadurabad (B). “F” denotes the Farakka barrage in India. The red line shows the border between India and Bangladesh.

60% of the total freshwater received by the BoB, of which 40% is supplied by the Ganga (hereafter (G))–Brahmaputra (hereafter (B)) river system alone [Sengupta *et al.*, 2006]. The Ganga–Brahmaputra River system (Figure 1a) is indeed the third largest freshwater outlet to the world ocean, with only the Amazon and the Congo surpassing the combined discharge of these two rivers [Dai *et al.*, 2009]. The Ganga extends across the great plains of northern India (Figure 1a). Once it enters Bangladesh, its name is Padma (Figure 1b). The Brahmaputra flows across the Himalayas (Figure 1a) and is called Jamuna in Bangladesh (Figure 1b). The Jamuna River joins the Padma River in Central Bangladesh and finally combines with the Meghna River to spread out onto a flat and wide floodplain, the largest river delta in the world [Chowdhury and Sato, 1996], before flowing into the Bay of Bengal (Figure 1b). In the following, we will use the better-known names Ganga for the Ganga–Padma and Brahmaputra for the Brahmaputra–Jamuna. After their confluence, we will call the river Ganga–Brahmaputra.

[4] In general, public access to the latest river discharge observations in the area is restricted and, up to now, only coarse estimates of river runoff into the BoB based on seasonal climatologies of hydrological models were available [e.g. Dai and Trenberth, 2002, and references therein]. This severely limits our ability to fully understand the climatic impacts of BoB runoff variations in the region, particularly at interannual time scales [Vinayachandran and Nanjundiah, 2009]. As a consequence, there is a need for access to comprehensive continental discharge estimates into the Bay of Bengal that can quantify the whole spectrum of variability from intraseasonal to interannual time scales.

[5] The primary archive for global in situ river discharge data is the Global Runoff Data Center [GRDC, 2009]. However, the most recent data available from this Center for the Ganga–Brahmaputra River is for 1992. Recently, effort has been made to characterize the variations of continental discharge to the World Oceans for more recent years. Using a combination of observations from in situ gauges and simu-

lations from a land surface model, Dai *et al.* [2009] released for community use a new data set for 1948–2004 of historical monthly streamflow for the world’s 925 largest ocean-reaching rivers. The data set includes estimates of river discharge of the Ganga–Brahmaputra River system into the Bay of Bengal until 2004.

[6] Hydrological observations in the Ganga–Brahmaputra River across Bangladesh have also been carried out by the Bangladesh Water Development Board since the early 1940s (<http://www.bwdb.gov.bd/>) and a new daily data set of Ganga and Brahmaputra river discharge observations from the 1950s to the beginning of the 2000s was recently released. Availability of such a long record is unprecedented for this part of the world and thus of extremely high value. Jian *et al.* [2009] for instance used the long-term, daily Ganga (1950–2003) and Brahmaputra (1956–2003) discharge time series to study the link between SST variability over the Indo-Pacific region and freshwater flux at intraseasonal and seasonal time scales.

[7] Using a subset of the same data over the 1992–1999 period (Durand, Impact of Ganga–Brahmaputra interannual discharge variations on Bay of Bengal salinity and temperature during 1992–1999 period, submitted to *Journal of Earth System Science*, 2010, revised; hereafter D10) forced an ocean general circulation model to assess the impact of G–B River discharge on the variability of Bay of Bengal Sea surface salinity and temperature. The study clearly showed that this impact is strong compared to other forcing factors in the northern part of the BoB and that extreme discharge anomalies are exported to the southern boundary of the Bay and can penetrate into the south-eastern Arabian Sea. In addition, this study pointed out two other results.

[8] 1. A direct comparison between the in situ discharge observations from the Bangladesh Water Development Board and the estimates from Dai *et al.* [2009] for 1992–1999 showed that, whereas both data sets are almost identical for 1992–1995, the agreement is poorer after 1996. Indeed after 1996, the Ganga river discharge estimates from Dai *et al.*

[2009] are not based on observations, but consist of synthetic discharge data constructed from numerical model outputs, which might have difficulties reproducing the interannual variability and large anomalous events.

[9] 2. There is a need of recent records of the Ganga-Brahmaputra River discharge, especially in the period after 2002, when the Argo project started providing routine salinity observations. Such a data set will help to calibrate and evaluate ocean numerical models. The study of Ganga-Brahmaputra impact on Bay of Bengal salinity is also timely given the recent launch in November 2009 of the satellite SMOS (Soil Moisture and Ocean Salinity) dedicated to monitor sea surface salinity over the Ocean [Kerr *et al.*, 2001].

[10] As already mentioned, the bulk of the available river discharge data for G-B covers the period up to 2004. It is hard to say whether updates to more recent years will be available in the near future, given that ground-based observations are difficult to obtain in the region.

[11] Over the last 20 years, satellite remote sensing techniques have been very useful for hydrologic investigations [Cazenave *et al.*, 2004; Alsdorf and Lettenmaier, 2003; Alsdorf *et al.*, 2007; Bjerklie *et al.*, 2003; Calmant *et al.*, 2008; Crétaux *et al.*, 2005; Papa *et al.*, 2006, 2008a, 2008b, 2010], and recent advances have demonstrated that some hydraulic variables can be measured reliably from satellites. In particular, satellite altimetry (TOPEX-Poseidon (T-P), ERS-2, and ENVISAT missions) has been used for systematic monitoring of water levels in large rivers, lakes, and floodplains, now providing a time series more than 15 years long [Birkett, 1998; Birkett *et al.*, 2002; Crétaux and Birkett, 2006; Calmant *et al.*, 2008; Frappart *et al.*, 2006, 2008]. In parallel, several studies have demonstrated the capability of using TOPEX-Poseidon satellite altimetry locally for estimating river discharge in large rivers (limited to rivers with a width of few kilometers), including the Ob River [Kouraev *et al.*, 2004], several sites along the Amazon River [Zakharova *et al.*, 2006; Leon *et al.*, 2006] or in Chari/Ouham confluence near the Lake Chad [Coe and Birkett, 2004]. Indeed, the advent of radar altimetry permits river water heights in large river basins to be correlated with in situ measurements of river discharge. For instance, the construction of empirical regression curves between altimetry-derived river water height and observed river discharge (called rating curves, details are given in section 3) can provide altimetry-based discharge estimates for times when in situ discharge observations are missing, or even, to extend forwards/backwards time series of river discharge. This technique has however several limitations [Alsdorf *et al.*, 2007]. First, the methodology strongly depends on the quality of the altimetry data themselves over continental water bodies (discussed in sections 2.2 and 2.3). Second, the methodology relies on the availability of some ground-based discharge measurements to determine the rating curves between altimetry-derived river water height and river discharge. As already seen, these in situ observations are not always available to the scientific community and when they are available, stream gauges are rarely located within the altimeter footprint (but usually within ~ 100 km), thus the relation between altimeter-derived river height and in situ discharge can suffer from differences in stream geomorphology between the in situ and satellite overpass locations. Another limitation is that, in order to

extend forwards/backwards time series of river discharge using altimeter measurements, the original relation of river height and discharge has to be assumed to be static over time (discussed in section 3); this assumption might not be valid over a long period of time. Finally, depending on the application, a major drawback in the use of altimetric measurements to monitor river stage and discharge is the temporal sampling rate. With a 10 day repeat cycle (T-P) or a 35 day repeat cycle (ERS-2/ENVISAT), satellite altimeters cannot compete with observations made daily or twice daily by in situ gauges, a frequency required to study local hydrological processes, to evaluate flood risk or for the management of water resources. Nevertheless, for studies related to climate, the use of radar altimetry can be extremely valuable as a complement to ground-based observations and can be advantageous because data are received continuously and are potentially available within a few days of measurement and therefore can provide valuable information where traditional gauge data can be irregular and difficult to obtain.

[12] Ideally, the goal for discharge data accuracy is within $\pm 5\%$ of the true value, but the community agrees that a 15%–20% accuracy is in general acceptable. Kouraev *et al.* [2004] over the Ob River and Zakharova *et al.* [2006] over the Amazon River showed that the errors of the estimated discharge using T-P data (at daily, monthly, or annual time scales) are well within the range of acceptable errors.

[13] The aim of the present study is twofold: first, to demonstrate the capability of using radar altimeters over the Ganga and the Brahmaputra Rivers; second, to produce a data set of monthly mean altimetry-derived comprehensive G-B River discharge at the river mouths during 1993–2008 with acceptable accuracy. This data set will be used in future studies to prescribe freshwater forcing flux into Indian Ocean circulation models. Hence, it is important to accurately monitor low flow and high flow seasons over a long period of time, as the ocean acts as an integrator of freshwater forcing flux, and thus, is likely to be influenced constantly by the fresh water forcing history during the few past seasons. Moreover, as for the monthly interval sampling, it corresponds both to the common time resolution of state-of-the-art discharge products [see, e.g., Dai *et al.*, 2009], and to the typical time scales satisfactorily resolved by ocean circulation models. Note that this data set will be also very useful as a source of evaluation for climate and hydrological models.

[14] Section 2 presents and discusses the data sets used in this study. They consist of in situ river height and discharge measurements, along with satellite altimetric river height time series. For the Ganga, we are able to present a direct comparison between in situ and altimetry-derived river height measurements. In section 3, we establish empirical relationships (rating curves) between satellite-derived water levels and in situ river discharge from gauging stations. In section 4, we use the rating curves for computing Ganga and Brahmaputra discharges and present monthly discharge estimates over the 16 year time span of T-P/ERS-2/ENVISAT altimetry data (1993–2008). The methodology is evaluated in various ways and discussed. We also evaluate our estimate over 2003–2008 (when in situ data are no longer available) by comparison with GPCP precipitation estimates and altimetry-derived river heights at other locations. Finally, in section 5, we present a basic approach to infer the total Ganga-Brahmaputra

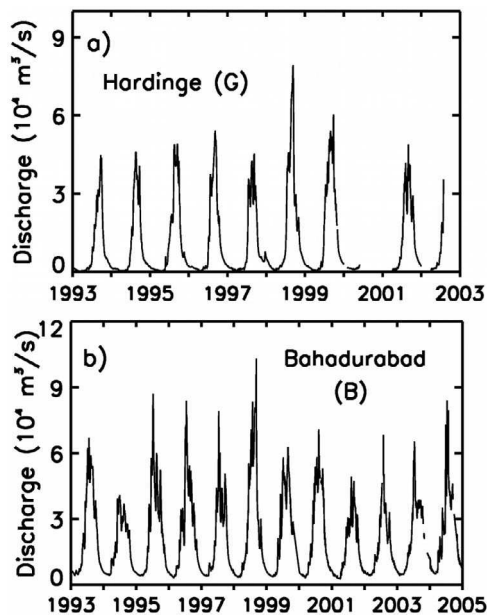


Figure 2. (a) Daily time series of in situ discharge of the Ganga River at Hardinge Bridge station. (b) Daily time series of in situ discharge of the Brahmaputra River at Bahadurabad station.

monthly discharge data set at the river mouths from the upstream estimate we produce and discuss its seasonal to interannual variability.

2. Data Sets and Evaluation

2.1. Ganga and Brahmaputra In Situ River Discharges

[15] We use hydrological observations in the Ganga and Brahmaputra Rivers in Bangladesh made by the Bangladesh Water Development Board (<http://www.bwdb.gov.bd/>). In particular, we have access for the present study to daily streamflow data collected at the two basin outlet stations before their confluence (Figures 1a and 1b): the Hardinge Bridge station (hereafter G, 24.07°N; 89.03°E) for the Ganga and the Bahadurabad station (hereafter B, 25.15°N; 89.70°E) for the Brahmaputra. Both stations lie close to the Bangladesh-India border.

[16] The discharge data are derived from water levels measured at staging stations and converted into discharge using stage-discharge relationships (rating curves, presented in section 3). In the following we call these data “in situ discharge,” although we point out that these are not direct discharge measurements. For the bulk of our data set, we do not have access to the original water level data used to infer the discharge (for 2007, we have 152 direct measurements of both water level and discharge, see section 2.3). The accuracy of these discharge measurements is not known; however even if it remains difficult to measure the depth and velocities, and consequently the true discharge of large and strong-flowing rivers like the Ganga and Brahmaputra [Chowdhury and Ward, 2004], typical accuracy of river discharge measurements is assumed to be in the range of 10%–20% [Fekete et al., 2000].

[17] Daily Ganga and Brahmaputra discharge data available for the study extend from 1993 to mid-2002 and 1993 to 2004, respectively, as shown in Figure 2. The Ganga river

discharge record has a significant gap from early 2000 through early 2001, as well as at the beginning of 2002. For the Brahmaputra data set, a few days in October 2003, the month of November 2003 and a few days in September 2004 are also not available. A detailed description of the 50 year daily discharge record for both rivers and the variations at intraseasonal and seasonal time scales is given by Jian et al. [2009], with a special emphasis on the 1990s.

[18] Both river discharge records displayed in Figure 2 show a large seasonal cycle and strong interannual variability with especially large year-to-year variations in their individual peak flows. The Ganga discharge at Hardinge is characterized by a low flow season from October/November to June, an increasing flow period starting in July and a maximum flow that occurs generally in August or September. The mean value for the 1993–2003 period is $\sim 11,000 \text{ m}^3/\text{s}$. During the high flow season the river discharge typically exceeds $30,000 \text{ m}^3/\text{s}$, with the August monthly average amounting to $39,400 \text{ m}^3/\text{s}$. The Brahmaputra discharge at Bahadurabad shows a low flow season from December to April, followed by an increasing flow period starting in May, reaching a peak flow generally in July. The 1993–2004 average value is $\sim 20,800 \text{ m}^3/\text{s}$. During the high flow season the river discharge generally shows values above $50,000 \text{ m}^3/\text{s}$ (except 1994 and 2001). The July monthly average value over the record is $\sim 54,600 \text{ m}^3/\text{s}$.

[19] In the following, the letter G will refer either to the Ganga River or the Hardinge station and the letter B will refer to the Brahmaputra River or the Bahadurabad station. We will call the discharge at Hardinge on the Ganga Q_G and the discharge at Bahadurabad on the Brahmaputra Q_B .

2.2. Satellite Altimetry Observations

[20] Satellite radar altimeters are initially designed to measure the ocean surface topography by providing along-track nadir measurements of water surface elevation. Radar altimetry entails vertical range measurements between the satellite and the Earth surface and the water level is given by the difference between the satellite orbit information and the range (or altimetric height) [Fu and Cazenave, 2001]. In parallel, they also became important tools to monitor ice sheet topography and mass balance [Rémy and Parouty, 2010], sea ice thickness, and land topography [Berry, 2000]. Moreover, radar altimeter water level data have long been shown to be precise enough for continental water studies and have been used for systematic monitoring of water levels of large rivers, lakes, and floodplains [Birkett, 1998; Birkett et al., 2002; Crétaux and Birkett, 2006; Calmant et al., 2008]. Altimetric observations over large rivers have been intensively evaluated in several regions against in situ gauge stations providing water level heights [Leon et al., 2006].

[21] There are various databases that provide time series of water stages in the great basins of the world [Calmant et al., 2008]. We use water levels coming from three altimeter satellites.

[22] 1. T-P-derived river and lake level heights from the HYDROWEB database [Crétaux et al., 2010], available at <http://www.legos.obs-mip.fr/en/soa/hydrologie/hydroweb/>. For T-P, this database provides consistent and accurate river level heights from 1993 to 2001, before the orbit of T-P was changed. The T-P orbit has a 10 day repeat cycle, meaning a measurement at the same location is available every 10 days

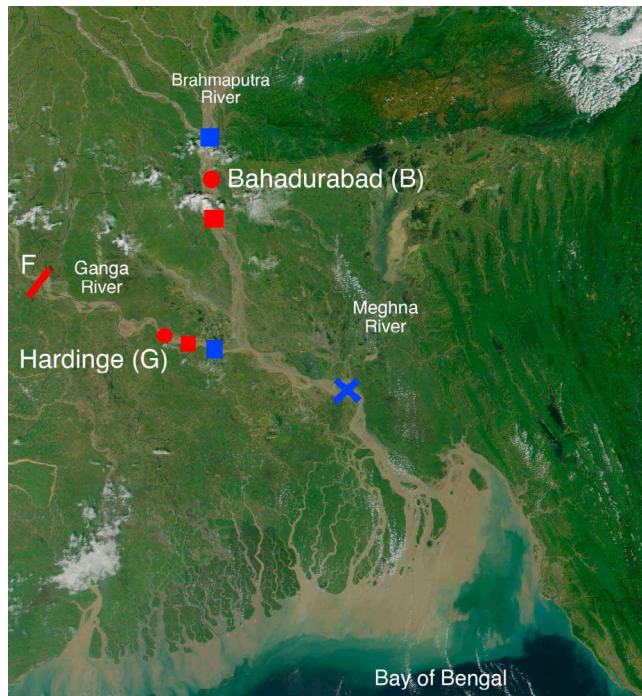


Figure 3. MODIS (Moderate Resolution Imaging Spectroradiometer) image of the region (for October 2001) with the location of the intersections between the altimeter ground tracks and each river (called virtual stations, red square for T-P, blue square for ERS-2/ENVISAT). The locations of the in situ discharge stations are displayed with red circles. F denotes the Indian Farakka barrage. The blue cross shows the location of the ENVISAT virtual station used in our analysis to evaluate the results (section 4.2.3).

(in fact 9.91 days). Radar altimetry is a profiling and not an imaging technique and for T-P the intertrack spacing at the equator is ~ 350 km. The follow-up mission of T-P, Jason-1, launched in 2001, has a different on-board processing and the additional filtering removed much of the altimeter data over continental surfaces and inland water bodies. Thus, it cannot be used for studies over the Ganga-Brahmaputra River.

[23] 2. ERS-2 derived river level height time series come from the ESA's River&Lake initiative, available at <http://tethys.eaprs.cse.dmu.ac.uk/RiverLake/shared/main> [Berry *et al.*, 1997, 2004]. ERS-2 covers the period 1995–2002 with a 35 day orbit repeat cycle providing an intertrack spacing at the equator of ~ 80 km.

[24] 3. ENVISAT-derived river level height time series is available from the HYDROWEB database. ENVISAT has the same orbital configuration as ERS-2. We use the measurements from 2003 to 2008.

[25] We refer to Crétaux *et al.* [2010], Berry *et al.* [1997, 2004, 2005], and Calmant *et al.* [2008] for a complete description of the satellites and the methodologies used to construct water level time series over large rivers, including the atmospheric corrections and the different algorithms, called trackers, used to process altimeter radar echoes over continental water bodies.

[26] Given the radar altimeters orbit configurations, there are several intersections between the satellites ground tracks and the Ganga and Brahmaputra rivers. These intersections are termed “virtual stations.” For our study, we selected for each satellite the nearest virtual stations to the Hardinge and Bahadurabad gauging stations. They are shown in Figure 3. Their position information, the satellite track number, their distance to the gauging station and the river width for high/low water stage at these locations are given in Table 1. As seen in Figure 3, all individual intersections between the satellite tracks and the rivers are located before the confluence of the two rivers. Also important, the Farakka barrage (F) in India (Figures 1b and 3), located about 80 km upstream of the station Hardinge, has no impact on our study as the altimeter virtual stations on the Ganga are also located downstream of the barrage.

[27] Note that when we use T-P data, the intersection between the satellite track and both rivers happens to be on the same track (231). This means that the T-P-derived water level observations over the Ganga and the Brahmaputra are made on the same day within a few seconds. For ERS-2/ENVISAT, the intersections between the satellite track and the two rivers are on different tracks. As a consequence, when a water level height is measured with ERS-2 over the Ganga, the water level height over the Brahmaputra is obtained 16 days later. Finally, note that, at the intersections between the satellites tracks and the river, the width of the channel (estimated from the GeoCover Landsat Thematic Mapper orthorectified mosaics available from the MrSID Image Server at <https://zulu.ssc.nasa.gov/mrsid/mrsid.pl>) is always larger for the Brahmaputra than for the Ganga (Table 1). This is also visible on the MODIS snapshot of the area for October 2001 shown in Figure 3. Given that the accuracy of altimeter-derived river level height is dependent, among other factors (see below and section 2.3), on the river width, we expect more accurate measurements over the Brahmaputra than over the Ganga.

[28] Figure 4 shows the times series of water level height for the Brahmaputra River using T-P (Figure 4a) and ERS-2/

Table 1. Description of the Virtual Stations (Intersections Between the Satellites Ground Tracks and the Rivers) for Each Satellite^a

	Virtual Station Coordinates (Latitude/Longitude)	Altimeter Track Number	Distance to the Gauging Station	River Width for Low/High Water Stage (km)
Ganga, T-P	23.92°N; 89.33°E	231	~ 25 km downstream of G	2/5
Ganga, ERS-2/ENVISAT	23.82°N; 89.52°E	337	~ 50 km downstream of G	2/6
Brahmaputra, T-P	24.74°N; 89.70°E	231	~ 40 km downstream of B	4/8
Brahmaputra, ERS-2/ENVISAT	25.72°N; 89.76°E	795	~ 60 km upstream of B	4/10

^aThe in situ gauging station for the Ganga is Hardinge (called G and located 24.07°N/89.03°E). The in situ gauging station for the Brahmaputra is Bahadurabad (called B and located 25.15°N/89.70°E).

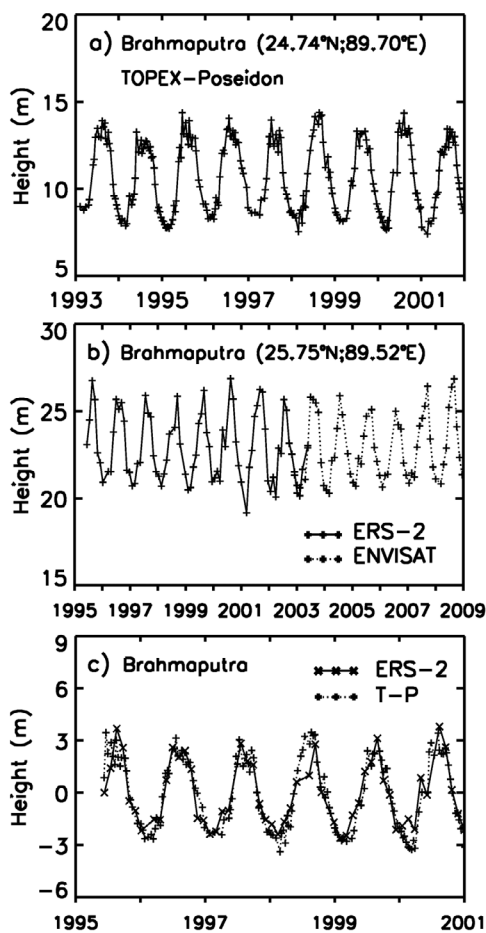


Figure 4. Time series of altimeter-derived river level height for the virtual stations of the Brahmaputra River (see Figure 3 and Table 1 for their locations). (a) The river level height every 10 days from T-P (plus signs with solid line) for 1993–2001. (b) The river level height every 35 days from ERS-2 (1995–2003, plus signs with solid line) and from ENVISAT (2003–2008, plus signs with dashed line). (c) The comparison for 1995–2001 of river level height every 10 days from T-P (plus signs with dashed line) and river level height every 35 days from ERS-2 (crosses with solid line). To make both variables comparable, their mean has been removed.

ENVISAT (Figure 4b) altimeters. Consistent with Figure 2, a large seasonal cycle with marked interannual variability is exhibited over the record. The peak-to-peak height variations can exceed 7 m. From December 2002 to May 2003, there are four dates where measurements are simultaneously available from ERS-2 and ENVISAT (Figure 4b). For those four observations, the mean difference between the water level height measured by each satellite is ~ 0.23 m (for instance, for the 6 January 2003, the difference is 0.43 m and, for 26 June 2003, the difference is 0.1 m). Figure 4c shows that, despite the fact that T-P and ERS-2 virtual stations are located ~ 100 km apart (Figure 3 and Table 1), both time series (their mean has been removed to make them comparable) are in good agreement and have a similar behavior in the peak-to-peak height variations (except during 1998 where ERS-2 shows a large discrepancy during the summer). For 1995–2001, the T-P-derived water level has a mean value of

10.83 m and a standard deviation (STD) of 2.03 m. For ERS-2, the mean value for 1995–2001 is 22.99 m and the STD is 1.92 m. The two satellites data sets thus show similar variability range. Note that, the difference in the mean height and in the absolute value of the water level is due to the fact that the water level data measured from space by radar altimeter refer first to an ellipsoid of reference and are then expressed with respect to a geoid model. In our case, both T-P and ERS-2 time series are constructed with reference to the EGM96 geoid model, and thus, the difference in the mean height is due to different values of the local geoid height at the locations of the two virtual stations. It is also important to point out that, in terms of single river level height measurements, there are several factors, beside the distance between the two virtual stations or the river width, that could introduce small differences between T-P and ERS-2 measurements [Crétaux *et al.*, 2010; Calmant *et al.*, 2008]: the use of a different tracker to retrieve the altimetric range (OCEAN tracker for T-P and ICE for ERS-2), a different precision of the satellite orbit or the use of different data sets to correct the height estimates from atmospheric contributions (water vapor corrections, ionospheric corrections).

[29] In the following, we use the following nomenclature to refer to the altimetry-derived river height from T-P, ERS-2, and ENVISAT over the Ganga and the Brahmaputra: $H_{T-P/G}$, $H_{T-P/B}$, $H_{ERS-2/G}$, $H_{ERS-2/B}$, $H_{ENV/G}$, and $H_{ENV/B}$, respectively.

2.3. Evaluation

[30] The estimated accuracy of the satellite altimetry measurements is estimated to be ~ 0.03 m over oceans and large, wind-roughened, unfrozen lakes [Crétaux *et al.*, 2010]. Over rivers, the accuracy depends on the width of the river, on the morphology of the banks and on the surface roughness of the target. The accuracy also varies depending on the altimeter specifics and data processing (for instance, ice mode range bin for ERS-2 is four times wider than for ocean mode range bin for T-P). Overall, the typical accuracy is 10–20 cm over large rivers such as the Amazon [Birkett *et al.*, 2002; Frappart *et al.*, 2006]. The accuracy may be further reduced over narrower rivers and/or in presence of vegetation [Calmant *et al.*, 2008]. These estimates are accepted by the community but the actual accuracy might vary a lot with the target.

[31] In addition to the data presented in section 2.1, we also have access to 152 direct in situ water level measurements at Hardinge made infrequently during 2007. Figure 5 compares these with $H_{ENV/G}$ for nine different points. $H_{ENV/G}$ are obtained within ± 3 days of the date at which the in situ river levels were measured. These nine points represent a fair sample of the seasonal variability through a year with the water level varying by ~ 8 m between the low and high water stages. Figure 5 clearly shows good agreement between the two data sets with a correlation of 0.96 ($p < 0.01$). The standard error is 0.26 m and is in the typical range of accuracy over large rivers. This comparison, even if made with a small data sample, covers the entire set of possible hydraulic regimes (low and high flow seasons). It thus provides confidence in using altimeter-derived water level over the Ganga-Brahmaputra region.

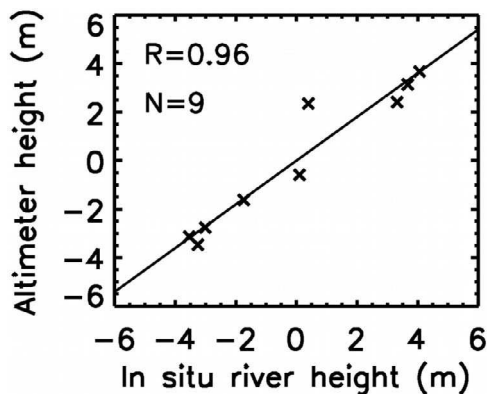


Figure 5. Scatterplot of the altimeter-derived river heights (from ENVISAT) versus the in situ river height over the Ganga in 2007. To make both variables comparable, their mean has been removed. The linear correlation coefficient (R) and the number of points (N) are indicated. The solid line shows the linear regression between both variables.

2.4. Precipitation Data Set

[32] In order to further evaluate our various estimates (sections 4 and 5) when in situ discharge observations are no longer available or when we upscale the discharge at the river mouths, we will compare them with precipitation over the Ganga and Brahmaputra watersheds estimated by the Global Precipitation Climatology Project (GPCP). GPCP, established in 1986 by the World Climate Research Program, provides data that quantify the distribution of precipitation over the globe [Adler *et al.*, 2003]. We use the Satellite-Gauge Combined Precipitation Data product of GPCP Version 2.1 data (monthly means from 1993 to 2008) with a spatial resolution of 2.5° in latitude and longitude. Over land surfaces, the uncertainty in the rate estimates from GPCP is generally lower than over the oceans due to the in situ gauge input (in addition to satellite) from the GPCC (Global Precipitation Climatology Center). Over land, validation experiments have been conducted in a variety of locations worldwide and the results suggest that, while there are known problems in regions of persistent convective precipitation, non-precipitating cirrus or regions of complex terrain, the estimated uncertainties range between 10% and 30% [Adler *et al.*, 2003].

3. Rating Curves

[33] In hydrology, the river discharge is routinely determined from river height measurements through a functional relation between the two quantities [Rantz *et al.*, 1982]. Such a relation is called the stage-discharge rating or rating curve. This relationship is specific to each gauging station and its development is regulated by different national and international standards. In practice, for one gauging station, there could be several relationships corresponding to different hydrological regimes such as low and high water stages or to rising and falling flooding periods [Kouraev *et al.*, 2004]. For instance, if the level-discharge relation shows highly scattered values, a detailed analysis of the relation is required and the data are split into subseries for different

seasons and/or different level ranges, and then are subjected to separate processing. However, over large rivers, such as the Amazon, where the complex stage-discharge relationships at Óbidos were evaluated, it was demonstrated that the uncertainties resulting from the use of a single rating curve are small compared with the other sources of error [Callède *et al.*, 2001].

[34] Figure 6 shows an example of a rating curve (relating river height (H) and river discharge (Q), hereafter called H - Q diagrams) for the Hardinge gauging station over the Ganga. This diagram is constructed using the simultaneous direct daily measurements of river height and river discharge during 2007. Once the relationship between the two variables is established, the river discharge can be estimated solely by measurements of the river height. Our approach uses this technique, but with river levels measured by altimetry in order to filling missing ground-based measurements and to extend forwards discharge time series. It is important to note here that several factors can influence differently over time the relation of stage to discharge and thus can alter gradually or abruptly the rating curve equation. These factors include the dynamics of the river bed itself, but also anthropic factors such as land use change, withdrawal for water use, or new contributions from artificial water storage reservoirs. In practice, the reinstallation of gauges and related bathymetric surveys can frequently be required and the rating curve has to be recalibrated with appropriate frequency. This is particularly important for rivers such as the Ganga and the Brahmaputra rivers, which carry huge volumes of flood water and sediments and may experience morphological changes. However, Mirza [2003] studied the evolution of the rating curves at Hardinge and Bahadurabad from 1966 to 1992 and showed that the Ganga and Brahmaputra rivers were in dynamic equilibrium during this period and that the rating curves previously developed in 1966 were still valid to at least 1992.

[35] Two different approaches can be considered to retrieve the river discharge using the satellite-derived water level data. One approach would use the official rating curve for a given point. For instance, it should be possible to establish the relationship between in situ and altimetry-derived water level measurements and then apply the rating

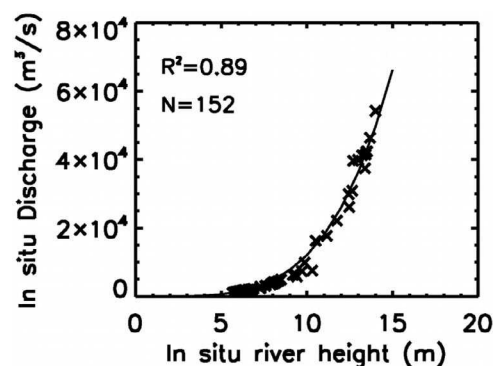


Figure 6. Scatterplot for 152 measurements during 2007 showing the relationship (rating curve) between in situ river height and in situ river discharge for the Ganga at Hardinge. The solid line is the power law regression between the two variables.

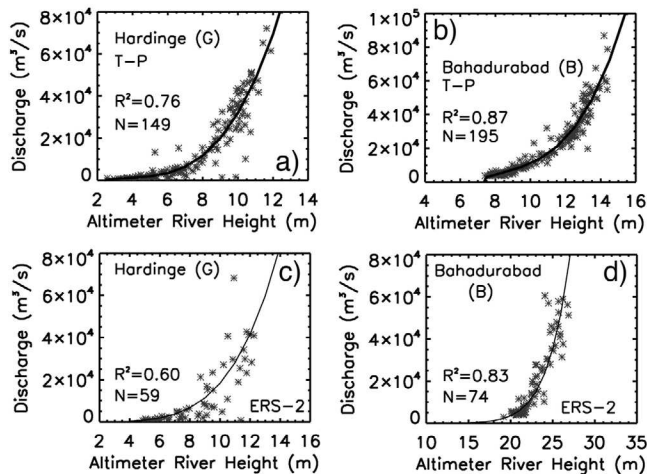


Figure 7. Scatterplots of in situ river discharge observations versus altimeter-based river height measurements showing the relationship (rating curve) between the two variables (see text for details): (a) for Hardinge, Ganga using T-P; (b) for Bahadurabad, Brahmaputra using T-P; (c) for Hardinge, using ERS-2; and (d) for Bahadurabad using ERS-2. The number of points (N) is indicated. The solid lines show the regression relation.

curves [Coe and Birkett, 2004]. However since we have access neither to the official rating curves for Hardinge and Bahadurabad nor to long time series of in situ water level measurements overlapping the satellite altimeters measurements, we use the alternative approach of establishing direct relationships between the altimeter-derived water levels at the satellite-river intersection and the in situ observed discharges at G and B. This approach was successfully used in several other studies using T-P data [Kouraev et al., 2004; Zakharova et al., 2006].

[36] The H - Q diagrams, using simultaneous (same day) measurements between altimetry-derived water level height and in situ river discharge, are presented in Figure 7. Figure 7 shows the rating curves between (1) $H_{T-P/G}$ and Q_G for 1993–2001 (Figure 7a, hereafter $H_{T-P/G}-Q_G$), (2) $H_{T-P/B}$ and Q_B (Figure 7b, hereafter $H_{T-P/B}-Q_B$) for 1993–2001, (3) $H_{ERS-2/G}$ and Q_G for 1995–2002 (Figure 7c, hereafter $H_{ERS-2/G}-Q_G$), and (4) $H_{ERS-2/B}$ and Q_B for 1995–2002 (Figure 7d, hereafter $H_{ERS-2/B}-Q_B$). Each H - Q relationship in Figure 7 shows the typical pattern of rating curves as in Figure 6. We note that, irrespective of satellite, the coefficient of determination R^2 is always less for Hardinge than for Bahadurabad. This might be explained by the fact that the width of river is less for the Ganga than the Brahmaputra (Table 1), which might result in less accurate altimetry height measurements of contamination of the radar signal by the presence of dry land in the satellite field of view. The $H_{ERS-2/G}-Q_G$ plot for the Hardinge station is the most scattered (Figure 7c). For this particular case, we tried to separate the data into different regimes, i.e., a rising period and a falling period [Kouraev et al., 2004], as the shape of the scatterplot suggests a phenomenon of hysteresis. In this case, discharge values at the same level could be higher during the period of falling flood than rising flood. However

this attempt was not successful and we argue that this larger dispersion is mainly caused by less accurate $H_{ERS-2/G}$ measurements at this particular point. This could be due to several factors, such as the contamination of the radar signal by the presence of dry land in the satellite field of view even during the high water season (the ice mode range bin for ERS-2 is 4 times wider than the ocean mode range bin for T-P). Moreover, both virtual stations for ERS-2 are located farther from the gauging stations than the T-P virtual stations, which might result in larger differences in local hydrological regimes and introduce different variations of water level.

[37] For each H - Q diagram, a single relationship is considered and a regression analysis is performed in order to obtain the best fitting rating curves. $H_{T-P/B}-Q_B$ and $H_{T-P/G}-Q_G$ are approximated by polynomial functions. $H_{ERS-2/G}-Q_G$ and $H_{ERS-2/B}-Q_B$ are approximated by power law functions.

4. Ganga and Brahmaputra River Discharge From Altimetry

4.1. Instantaneous Discharge Estimates

[38] T-P-derived discharge time series with a 10 day temporal sampling interval for Hardinge ($Q_{T-P/G}$) and for Bahadurabad ($Q_{T-P/B}$) are presented in Figures 8a and 8b and compared with daily in situ discharge measurements for both stations. Figures 8c and 8d show the ERS-2-derived 35 day discharge time series for the period 1995–2002 for Hardinge ($Q_{ERS-2/G}$) and for Bahadurabad ($Q_{ERS-2/B}$), as well as the ENVISAT-derived 35 day discharge time series for the period 2003–2008 for both stations ($Q_{ENV/G}$ and $Q_{ENV/B}$). Daily in situ discharge measurements are also shown. $Q_{ENV/G}$ and $Q_{ENV/B}$ are estimated using the rating curves $H_{ERS-2/G}-Q_G$ and $H_{ERS-2/B}-Q_B$ and the river level heights from ENVISAT $H_{ENV-2/G}$ and $H_{ENV-2/B}$. We assume here that the rating curve equations $H_{ERS-2/G}-Q_G$ and $H_{ERS-2/B}-Q_B$ remain valid for 2003–2008 (see section 3). Moreover, before using $H_{ENV-2/G}$ and $H_{ENV-2/B}$, we adjusted these time series to the ERS-2 ones by removing the difference of their means. Figure 9 shows the residuals for T-P and ERS-2-derived discharges for G and B (differences between altimetry-derived discharge and simultaneous in situ discharges, expressed as percent of the in situ discharge value) as a function of in situ discharge values.

[39] The best results are obtained for the Bahadurabad station using T-P (Figures 8b and 9b). Figure 8b clearly shows excellent agreement between the satellite-derived discharge and the in situ discharge in the seasonal timing of the various stages of the hydrological regime (seasonal low/high water flow) as well as in the interannual variability of the peak flow. For this station, $Q_{T-P/B}$ compared to Q_B gives a correlation of 0.97 ($n = 195$, Figure 8b). For each year, the low flow season and the high flow season are well depicted. The year-to-year variations are also in good agreement with the in situ observations, with for instance, larger discharge values obtained during the high flow seasons of 1996, 1998 and 2000. For this station, Figure 9b shows that the residual error for individual 10 day discharge is generally less than $\pm 25\%$ of the in situ discharge. More than 60% of the $Q_{T-P/B}$ are within 15% of in situ Q_B and the mean error (defined as the mean of absolute value of the residuals) of daily $Q_{T-P/B}$ is $\sim 15\%$. The errors on the estimated daily discharge

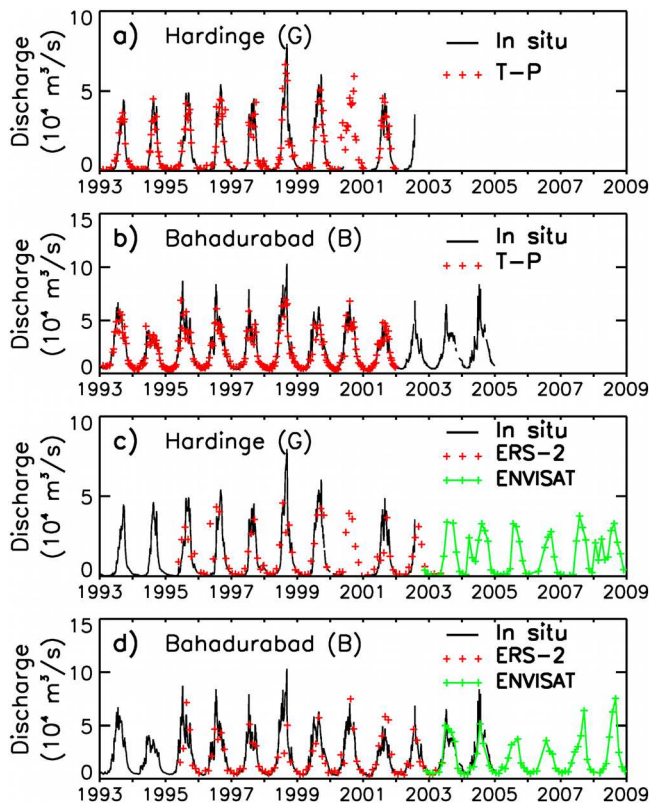


Figure 8. Time series of satellite altimeter-derived discharges and in situ observed discharges. (a) River discharges from T-P (red plus signs) and from in situ observations (solid black line) for Hardinge, Ganga. (b) River discharges from T-P (red plus signs) and from in situ observations (solid black line) for Bahadurabad, Brahmaputra. (c) River discharges from ERS-2 (red plus signs) and from ENVISAT (green plus signs) and from in situ observations (solid black line) for Hardinge, Ganga. The green line connecting ENVISAT-derived discharge estimates is used for visual purposes. (d) River discharges from ERS-2 (red plus signs) and from ENVISAT (green plus signs and green line) and from in situ observations (solid black line) for Bahadurabad, Brahmaputra.

derived from T-P for Bahadurabad are well within the range (10%–20%) of errors acceptable for discharge measurements. The standard deviation of the residuals is $4714 \text{ m}^3/\text{s}$ and the standard error of the estimates for the 195 daily discharge calculated is about $340 \text{ m}^3/\text{s}$, which amounts to 1.6% of the mean of Q_B over the record. Over the long term, the average value of $Q_{T-P/B}$ for 1993–2001 is $\sim 21,700 \text{ m}^3/\text{s}$, which is a difference of $600 \text{ m}^3/\text{s}$ or 2.8% with the 1993–2001 average value of Q_B using all in situ data ($21,100 \text{ m}^3/\text{s}$).

[40] Good agreement in the seasonal and interannual variations between satellite-derived discharge and in situ discharge (Figure 8a), with low residuals (Figure 9a), is also obtained when estimating $Q_{T-P/G}$ at Hardinge station. $Q_{T-P/G}$ compared to Q_G gives a correlation of 0.94 ($n = 149$) and the standard deviation of the residual is about $6000 \text{ m}^3/\text{s}$. The large events during the high flow season in 1998 and in 1999 are particularly well depicted (Figure 8a). Figure 9a shows that the residual error for individual daily discharge is gen-

erally less than 25% of the absolute value of the in situ discharge for discharge rates of greater than about $10,000 \text{ m}^3/\text{s}$. Note that during the winter season, the Ganga discharge can have values lower than $1000 \text{ m}^3/\text{s}$ and Figure 9a shows that for discharge rates below about $5000 \text{ m}^3/\text{s}$ the residual error can increase to greater than 40% in relative values. The mean error of daily $Q_{T-P/B}$ is $\sim 31\%$, but is reduced to 19%, in the range of acceptable accuracy for discharge measurements, when only discharges over $5000 \text{ m}^3/\text{s}$ are considered. The increased error at low discharge values illustrates the difficulties of the altimeter to accurately determine low discharge during the dry season when the river is narrower ($\sim 2 \text{ km}$ for the Ganga during low water season), as has been observed in other areas [Zakharova *et al.*, 2006].

[41] In Figures 8c and 8d, ERS-2-based discharges $Q_{ERS-2/G}$ and $Q_{ERS-2/B}$ every 35 days for 1995–2003, also show overall good agreement in the timing of the various stages of the hydrological regime, with low and high discharge seasons well depicted. For Hardinge, $Q_{ERS-2/G}$ compared to Q_G gives a correlation of 0.85 ($n = 59$). For Bahadurabad, the correlation is 0.89 ($n = 74$). As expected from Figure 7, $Q_{ERS-2/G}$ and $Q_{ERS-2/B}$ have the largest errors (Figures 9c and 9d), the standard deviation of the residuals reaching $9050 \text{ m}^3/\text{s}$ for Hardinge and $8300 \text{ m}^3/\text{s}$ for Bahadurabad. The mean error of daily $Q_{ERS-2/G}$ is $\sim 36\%$ and 29% for $Q_{ERS-2/B}$, which are a little above the range of acceptable accuracy. However, we will see in the next section that these errors are generally uncorrelated in time and therefore greatly reduced in monthly means or when only the high discharge season is considered.

[42] To assess the robustness of the altimetry-derived discharge using the rating curves, we tested the sensitivity of the rating curve estimates themselves. For instance, using T-P river heights and the in situ river discharge for Bahadurabad, we removed the year 1993 from the in situ observational record. We then constructed the diagram $H_{T-P/B}-Q_B$ using the data for the remaining years (1994–2001) and estimated the T-P-based river discharge for 1993 using the 1994–2001 rating curve and $H_{T-P/B}$ for 1993. This estimate is then compared with the in situ discharge for 1993. The same computations were performed for each year of the record, for both stations and using T-P and ERS-2 river heights (not shown). The standard deviation of the residuals (when compared to in situ Q_G and Q_B) was found to be $\sim 5500 \text{ m}^3/\text{s}$ (Hardinge) and $\sim 4800 \text{ m}^3/\text{s}$ (Bahadurabad) when using T-P and $9900 \text{ m}^3/\text{s}$ (Hardinge) and $\sim 8500 \text{ m}^3/\text{s}$ (Bahadurabad) when using ERS-2. These values are the same order of magnitude as the standard deviation of the residuals calculated above when the entire record is used, and smaller than the year-to-year variability of the summer peak discharge. This confirms that the altimetry-based rating curves can be used with confidence to retrieve river discharge variations for periods when in situ data are not available to construct the rating curves. In particular, this supports our extension of the time series over 2003–2008 for both stations using ERS-2 and ENVISAT and the rating curves $H_{ERS-2/G}-Q_G$ and $H_{ERS-2/B}-Q_B$.

[43] Using $H_{ERS-2/G}-Q_G$ and $H_{ERS-2/B}-Q_B$ and the ENVISAT river level heights, ENVISAT-derived 35 day discharge time series for both stations ($Q_{ENV/G}$ and $Q_{ENV/B}$) are displayed in Figures 8a and 8b for the period 2003–2008. $Q_{ENV/G}$ and $Q_{ENV/B}$ have seasonal cycles similar to $Q_{ERS-2/G}$ and $Q_{ERS-2/B}$ with values the same order of magnitude. Note

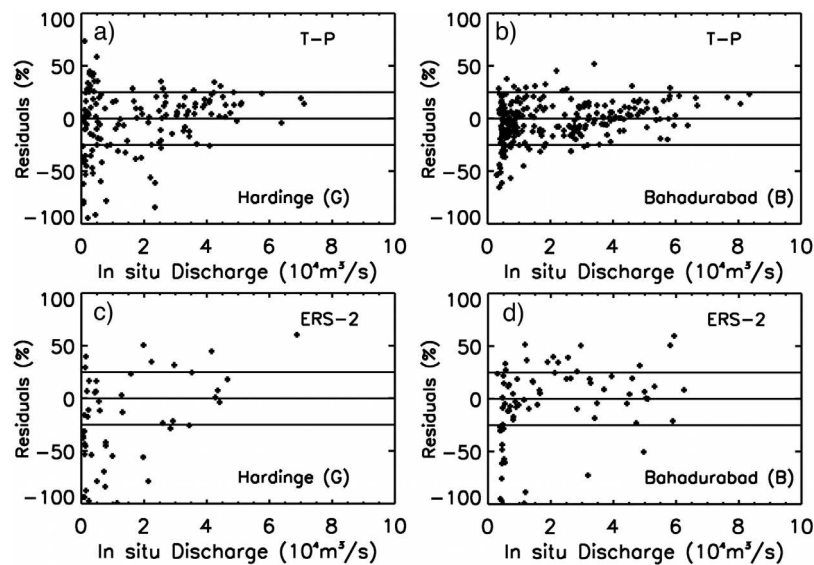


Figure 9. Percent residual as function of in situ discharge: scatter diagrams of error residuals of the altimeter-derived daily discharge (for T-P and ERS-2, shown as a percent of the in situ discharge) versus the in situ discharge at Hardinge, Ganga and Bahadurabad, Brahmaputra.

that $H_{ENV/B}$ were not used to compute the rating curve diagrams $H_{ERS-2/B}/Q_B$ (only $H_{ERS-2/B}$ were used) even though in situ river discharge for Bahadurabad are available for some portion of 2003 and 2004. This enables an independent evaluation of daily $Q_{ENV/B}$ against Q_B . The same analysis as in Figure 9 using $Q_{ENV/B}$ and Q_B for 2003 and 2004 (not shown) gives a standard deviation of the residuals about $4400 \text{ m}^3/\text{s}$. The mean error of daily $Q_{ENV/B}$ for 2003–2004 is $\sim 22\%$, which shows that daily discharge derived from ENVISAT for Bahadurabad are within the range of acceptable errors for discharge measurements.

[44] Figure 10 shows the discharge histograms using bins of $5000 \text{ m}^3/\text{s}$. The histograms for the in situ data are constructed using all the daily discharge observations over the common period with altimetry-based discharge. For instance, considering T-P at Bahadurabad (Figure 10b), the in situ discharge histogram is constructed using all the daily discharge available for 1993–2001. For altimetry-based discharge, the histograms are for $Q_{T-P/G}$ and $Q_{T-P/B}$ with a 10 day interval sampling interval and for $Q_{ERS-2/G}$ and $Q_{ERS-2/B}$ with a 35 day sampling interval. For the in situ discharge measurements at each station, we also constructed the histograms for the subsets of observations sampled at the same date as the altimetry-based estimates. Overall, in each panel of Figure 10, the histograms show similar patterns, the distribution of satellite-derived discharges generally fitting the distribution of in situ discharges. This is particularly true for both satellites at Bahadurabad (Figures 10b and 10d). All satellite estimates capture the large fraction of the river discharge values during the low flow season (positive skew). Although relative errors are important in low flow season, as previously discussed, absolute errors are small and are integrated here in the $5000 \text{ m}^3/\text{s}$ bin. All data set agree well for discharge values between $10,000$ and $50,000 \text{ m}^3/\text{s}$. For Hardinge using T-P, the discharge values between $10,000$ and $40,000 \text{ m}^3/\text{s}$ show a ratio larger than the in situ measurements because of the number of missing satellite data during the low flow season.

The histograms also show that events with extreme discharges ($>50,000 \text{ m}^3/\text{s}$ for Hardinge and $>65,000 \text{ m}^3/\text{s}$ for Bahadurabad) represent small fractions of the total number of observations. Using all daily in situ data, $50,000 \text{ m}^3/\text{s}$ for Hardinge and $65,000 \text{ m}^3/\text{s}$ for Bahadurabad are at the 97th percentile. Using T-P discharge estimates, $50,000 \text{ m}^3/\text{s}$ for Hardinge is at the 96th percentile and $65,000 \text{ m}^3/\text{s}$ for Bahadurabad is at the 98th percentile. Using ERS-2 discharge estimates, $50,000 \text{ m}^3/\text{s}$ for Hardinge is at the 99th percentile and $65,000 \text{ m}^3/\text{s}$ for Bahadurabad is at the 97th percentile.

4.2. Ganga-Brahmaputra Monthly Discharge Estimates

[45] Analysis of the river discharge data set show that there is a phase locking of the interannual variability on the seasonal cycle, with discharge anomalies occurring mainly during the summer period, i.e., during the high flow season. Hence, before computing the monthly mean time series, we investigate two further points dedicated to this season: (1) evaluate the altimetry-based discharge data during the high water flow season for each river and (2) quantify the effects of the 10 day and 35 day temporal sampling when estimating a mean discharge around the yearly peak discharge.

4.2.1. Altimetry-Based Discharge Data During the High Water Flow Season

[46] As seen in the previous section, all our river discharge time series reconstructed using altimetry generally show excellent agreement in the timing of the various stages of the hydrological regime. The satellite-derived discharges clearly indicate the low discharge season (even though the relative errors are important when the flow is really low, absolute errors are small) and the high flow season. However, it is obvious that increased daily relative errors are obtained during the low discharge periods. During these periods, the river is narrower, the spatial length of the altimeter-river crossing is thus smaller than during the period of high water

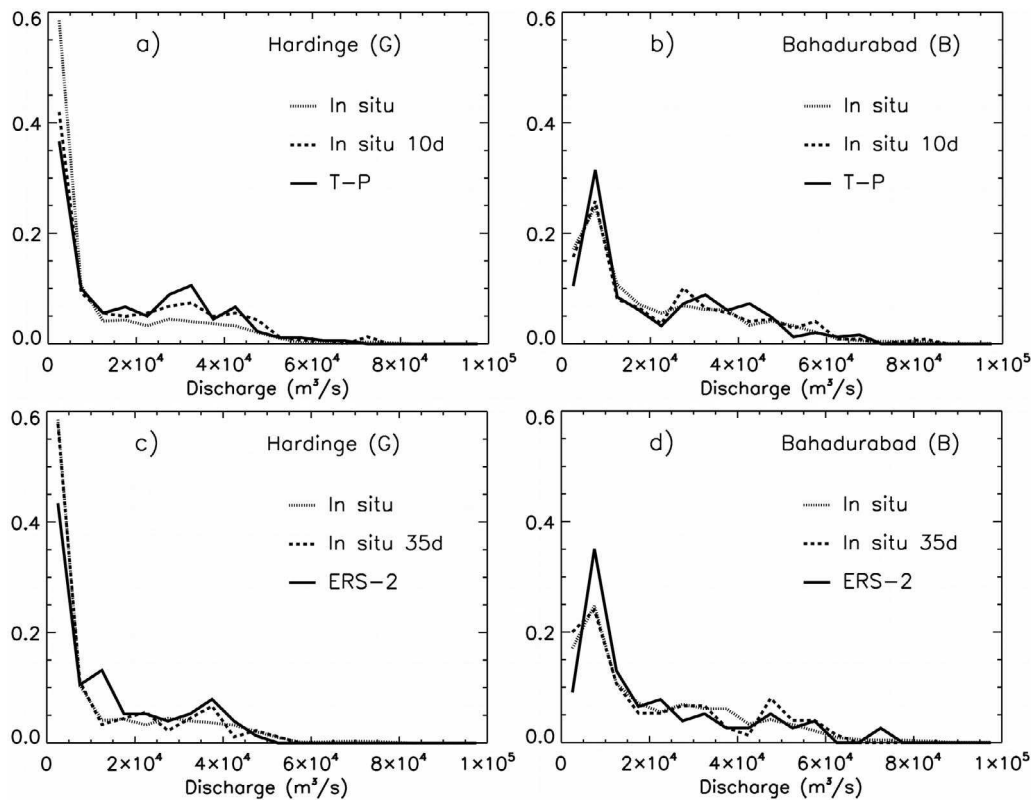


Figure 10. Histograms (bin of $5000 \text{ m}^3/\text{s}$, each tally is divided by the total number of observations) of river discharges from in situ measurements and as estimated by radar altimetry with a temporal sampling interval of 10 days for T-P and 35 days for ERS-2. To construct the in situ discharge histograms, all daily observations available during the overlapping period with each satellite are used. The histograms using a subset of the in situ discharge measurements sampled at the same date as the altimetry-based estimates (10 day and 35 day) are also displayed. (a) Histograms for T-P-derived (black line) and in situ discharges (daily in dotted line and 10 day samples in dashed line) for Hardinge. (b) Histograms for T-P-derived (black line) and in situ discharges (daily in dotted line and 10 day samples in dashed line) for Bahadurabad. (c) Histograms for ERS-2-derived (black line) and in situ discharges (daily in dotted line and 35 day samples in dashed line) for Hardinge. (d) Histograms for ERS-2-derived (black line) and in situ discharges (daily in dotted line and 35 day samples in dashed line) for Bahadurabad.

flow. The radar signal also can be contaminated by the presence of dry land resulting in noisier and less accurate estimates of the river height (or even missing data because they did not meet the quality criteria).

[47] To assess the accuracy of the altimetry data for determination of discharge values during the high water flows, we have computed a mean high water flow discharge for each river from the altimetry-based discharge data. On the basis of in situ data analysis, the high water flow is from July to October for Hardinge and from May to November for Bahadurabad. The comparisons with the in situ mean discharge for the same periods are reported in Tables 2 and 3 for both stations.

[48] The mean differences between the T-P-derived and in situ discharges are low, about 8% for Hardinge (Table 2) and 5.5% for Bahadurabad (Table 3). Using ERS-2, the mean differences are 21.6% for Hardinge (Table 2) and 15.1% for Bahadurabad (Table 3). Using ENVISAT for 2003 and 2004 for Bahadurabad (not reported in a table), the mean difference between altimeter-derived and in situ discharges for high water flow averages is 11.5%. This evaluation shows that the

altimeter-derived discharges during the high water flows are well within the range of uncertainties acceptable for river discharge estimations.

[49] The largest error for Hardinge using T-P occurs in 1993 (24.5%). In 1993, we carefully checked the in situ discharge data and found that the beginning of high water flow season is delayed by about 3 weeks compared to other years. Knowing that the altimeter does not perform well during low flow episodes, we end up with an excess error for this year as compared to the rest of the record. Indeed, Q_G increases above $10,000 \text{ m}^3/\text{s}$ in the last days of July 1993, whereas for all the other years, Q_G is generally above $10,000 \text{ m}^3/\text{s}$ in early July. For 1993, reducing the high water flow season from the end of July to October decreases the error between $Q_{T-P/G}$ and Q_G to less than 12%. The largest error for Hardinge using ERS-2 is found in 1996 (44.8%) and can be explained by the fact that during this year half of ERS-2 data are missing with only two $Q_{ERS-2/G}$ estimates that can be computed.

[50] The largest error for Bahadurabad using T-P is found in 1999 (Table 3, 13.9%), which is also a year where T-P

Table 2. Mean Values During the High Flow Season (July to October) of River Discharges at Hardinge Station From Altimetry ($Q_{T-P/G}$ and $Q_{ERS-2/G}$) and In Situ Data and Errors (%) of Estimation^a

Discharge (m ³ /s) and Error	1993	1994	1995	1996	1997	1998	1999	2000	2001	2002
Q_G	22,070	24,430	28,330	28,800	25,270	38,800	37,630	–	27,480	–
$Q_{T-P/G}$	27,470 (9)	23,340 (12)	29,200 (10)	32,040 (12)	25,550 (10)	39,680 (9)	34,200 (8)	–	30,140 (11)	–
Error (%)	24.5	–4.4	3.1	11.2	1.1	2.3	–9.1	–	9.7	–
$Q_{ERS-2/G}$	–	–	22,130 (4)	41,700 (2)	22,120 (4)	34,990 (3)	34,720 (4)	–	18,320 (4)	24,980 (3)
Error (%)	–	–	–21.9	44.8	–12.5	–9.8	–7.7	–	–33.3	–

^aAll in situ Q_G over the high flood period are used. The number in bracket following the altimetry-derived discharge value gives the number of observations available to calculate the mean value.

has the largest number of missing data, with only 14 $Q_{T-P/B}$ computed, i.e., three measurements less than the average number of $Q_{T-P/B}$ computed during the high water season. Using ERS-2, $Q_{ERS-2/B}$ compared to Q_B (Table 3) shows large errors in 1998 (30.7%) and in 2001 (–50.7%). In August 1998, as seen in Figure 8b, $Q_{ERS-2/B}$ does not accurately capture the high discharge event and underestimates Q_B . In 2001, Figure 8b shows that $Q_{ERS-2/B}$ greatly overestimates Q_B in August and September, which results in a large error in the high water discharge estimates.

4.2.2. Effects of Temporal Sampling Around the Yearly Peak Discharge

[51] Before computing the monthly mean time series, we also investigate the effects of the 10 day and 35 day temporal sampling around the yearly peak discharge. With a coarse 35 day sampling interval, ERS-2 and ENVISAT may provide estimates of the discharge too far or too close to the peak time. For a more quantitative examination of this issue, we performed the following analysis for both rivers G and B using the in situ discharge data sets. The date of the peak flow is identified for each year in the in situ record. A sliding window of 35 days is applied to the record, starting 35 days before the peak flow and going to the peak flow date in each year. The window moves with 1 day steps; at each step, the average discharge is calculated using all 35 days in the window (the true mean) and using only the two end-points. The same calculation is done for all the years when in situ discharge is available. The difference (in percent of true mean) between the two means at each step is averaged over the years. The analysis is done for both stations and also with the 10 day window. The results are plotted in Figure 11 for the two stations.

[52] With the 10 day window, small differences are generally observed for Hardinge (Figure 11a). When one of the end-points is on the date of the peak flow (day = 0 for instance), the mean discharge using the two end-points

overestimates the true 10 day mean river discharge by only few percent. Moving the window forward shows that the differences (underestimates) are less than 10% reaching a maximum when the two samples bracket the peak flow date. The differences are larger for Bahadurabad with almost permanent underestimations of the 10 day mean discharge as soon as the peak flow is missed by one day. However, the differences are generally less than 10% with a maximum underestimation of 15%. For both stations, as expected, the differences are a little larger with the 35 day window. When one of the end-points is within ± 5 days of the date of the peak flow, the overestimation is in the order of 5%–20%. The maximum differences, when the two samples bracket the peak flow date, show an underestimation between 10% and 20%, the largest differences being for Bahadurabad. These results show that, for the Ganga and the Brahmaputra, even with a coarse 35 day interval sampling interval, the underestimation or overestimation of the true mean discharge never exceeds 20%, which is within the range of uncertainties acceptable for river discharge estimations. The uncertainties related to the effects of altimeter temporal sampling around the yearly peak discharge might vary greatly from river to river and we suggest that an analysis similar to the one we used here should be performed in future studies that will investigate the possibility of retrieving river discharge using radar altimeters over other river basins.

4.2.3. Monthly Discharge Estimates for the Ganga, the Brahmaputra, and Their Total

[53] Monthly discharges for G and B for 1993–2008 are determined from multiple radar altimeters. Since T-P performs significantly better than ERS-2 (section 4.1), we use the $Q_{T-P/G}$ and $Q_{T-P/B}$ for 1993–2001. For 2002, we use $Q_{ERS-2/G}$ and $Q_{ERS-2/B}$ and for 2003–2008, we use $Q_{ENV/G}$ and $Q_{ENV/B}$. No adjustment between the time series is made. The altimetry-derived discharge for 1993–2008 is called $Q_{ALT/G}$ for the Ganga and $Q_{ALT/B}$ for the Brahmaputra.

Table 3. Mean Values During the High Flow Season (May to November) of River Discharges at Bahadurabad Station From Altimetry ($Q_{T-P/B}$ and $Q_{ERS-2/B}$) and In Situ Data and Errors (%) of Estimation^a

Discharge (m ³ /s) and Error	1993	1994	1995	1996	1997	1998	1999	2000	2001	2002
Q_B	33,930	24,330	35,300	34,580	27,990	39,660	33,620	32,420	24,420	22,960
$Q_{T-P/B}$	35,760 (16)	25,140 (19)	35,960 (16)	34,390 (18)	26,960 (16)	37,780 (15)	28,930 (14)	33,200 (17)	27,650 (21)	–
Error (%)	5.4	3.3	1.9	–0.6	–3.7	–4.8	–13.9	2.42	13.2	–
$Q_{ERS-2/B}$	–	–	34,840 (5)	30,600 (6)	27,370 (5)	27,480 (4)	27,350 (6)	30,700 (6)	36,800 (6)	22,850 (6)
Error (%)	–	–	–1.3	–11.5	–2.2	–30.7	–18.6	–5.6	50.7	–0.5

^aAll in situ Q_B over the high flood period are used. The number in bracket following the altimetry-derived discharge value gives the number of observations available to calculate the mean value.

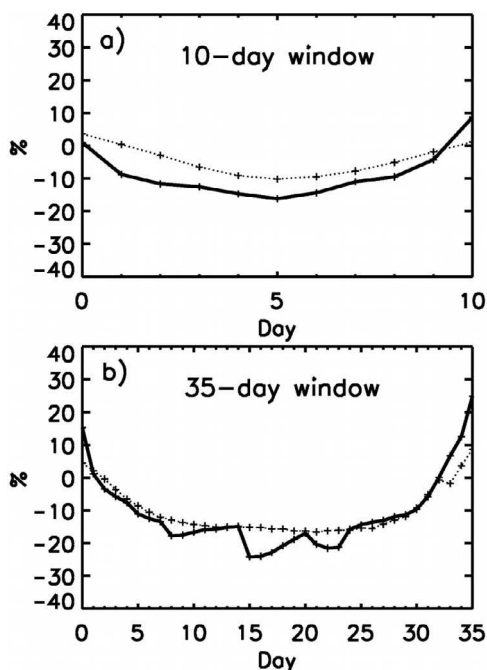


Figure 11. Quantitative evaluation of the (a) 10 day and (b) 35 day sampling intervals in the estimation of mean river discharge around the yearly peak flow (see text for details and the method). In situ data at Hardinge, Ganga (dotted line) and at Bahadurabad, Brahmaputra (solid line) are used. The x axis values represent the lower endpoint of a 10 day or 35 day sliding window. For 0, the lower end-point of the window is 35 days (10 days) before the peak flow and the upper end-point is on the day of the peak discharge. The y axis represents for each step the average difference over the years between the average discharge calculated using only the two end-points and the true mean discharge calculated using all 35 days (10 days) in the window. The y axis values are expressed in percent of true mean.

For the discharges derived from T-P (10 day temporal sampling interval, 1993–2001), the monthly mean discharge is obtained by averaging all available daily discharges from T-P within a month. For ERS-2 and ENVISAT, we assume that the retrieved discharge for a particular month is given by the sample within this month regardless of the day of the month. Missing months are filled by linear interpolation. When two or more consecutive months are missing (a few cases in winter during the low discharge period), we assume the climatological mean (or zero anomaly) for these months. For Hardinge station, we also excluded from the analysis three consecutive months in 2008 (January, February, and March) and replaced them by the monthly climatology. As seen in Figure 8a, ENVISAT-based estimates for Hardinge in the beginning of 2008 provide river discharges above 20,000 m^3/s ($H_{\text{ENV}/\text{G}}$ are more than 5 m above normal for these months), which can plausibly be assumed to be unreal. We carefully checked GPCP rainfall estimates over the Ganga watershed and found no anomaly during the fall of 2007 and the winter of 2008.

[54] The derived time series of monthly river discharge for the Ganga at Hardinge ($Q_{\text{ALT}/\text{G}}$) and for the Brahmaputra at Bahadurabad ($Q_{\text{ALT}/\text{B}}$) for the period 1993–2008 are displayed in Figure 12, along with the monthly mean time series of in situ river discharge. Figure 12c shows an estimate of the total discharge of the combined rivers G+B (hereafter $Q_{\text{ALT}/\text{G+B}}$) obtained by summing the two individual discharges and compared to the total discharge of the combined rivers G+B from in situ data ($Q_{\text{G+B}}$, obtained by summing the two individual discharges Q_{G} and Q_{B}). The residuals (the difference between $Q_{\text{ALT}/\text{G+B}}$ and $Q_{\text{G+B}}$) is also shown. The mean annual discharges $Q_{\text{ALT}/\text{G}}$, $Q_{\text{ALT}/\text{B}}$ and $Q_{\text{ALT}/\text{G+B}}$ for each year between 1993 and 2008 are given in Table 4 along with a comparison with the in situ mean annual water flow (Q_{G} , Q_{B} , and $Q_{\text{G+B}}$).

[55] Figure 12 shows that the monthly satellite and in situ river discharges agree well in the timing of the various stages of the hydrological regime and in the interannual variability. In particular, from Figure 12c, we find that more than 70% of the $Q_{\text{ALT}/\text{G+B}}$ values are within 15% of in situ $Q_{\text{G+B}}$ values; the standard deviation of the residuals (green curve) is $\sim 2700 \text{ m}^3/\text{s}$ and the mean error (defined as the mean of absolute value of the residuals) of monthly $Q_{\text{ALT}/\text{G+B}}$ is $\sim 17\%$. This result shows that the altimeter-derived monthly discharge meets the requirements of acceptable accuracy

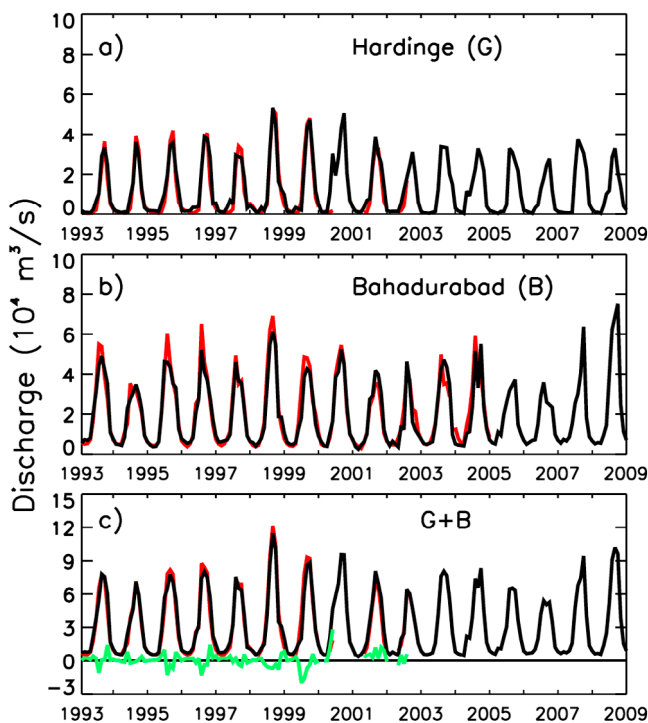


Figure 12. Time series of monthly river discharges derived from radar altimetry 1993–2008 (black line) and from in situ streamflow (red line). (a) For the Ganga at Hardinge (in situ data available from 1993 to mid-2002). (b) For the Brahmaputra at Bahadurabad (in situ data available from 1993 to mid-2004). (c) For the combined discharge of the two rivers G+B (in situ data available from 1993 to mid-2002). The green curve shows the residuals (the difference between the combined G+B discharge from altimetry and the in situ discharge).

Table 4. Mean Annual Values of River Discharge From Altimetry and In Situ Data at Hardinge ($Q_{ALT/G}$ and Q_G), Bahadurabad ($Q_{ALT/B}$ and Q_B), the Combined Discharge of the Two Rivers G+B ($Q_{ALT/G+B}$ and Q_{G+B}), and Errors of Estimations^a

Discharge (m ³ /s) and Error	1993	1994	1995	1996	1997	1998	1999	2000	2001	2002	2003	2004	2005	2006	2007	2008
Q_G	8520	9320	11,120	11,150	9950	15,390	14,540	—	—	—	—	—	—	—	—	—
$Q_{ALT/G}$	9980	9420	12,290	12,870	10,940	15,640	14,380	18,050	13,080	10,330	12,880	12,620	11,110	9090	13,170	10,940
Error (%)	17.1	1.1	10.5	15.4	9.9	1.5	-1.1	—	—	—	—	—	—	—	—	—
Q_B	22,360	16,980	22,850	22,830	18,770	25,620	22,100	21,990	15,930	16,630	20,880	22,950	—	—	—	—
$Q_{ALT/B}$	22,360	17,240	22,070	21,620	18,290	24,190	19,000	21,610	17,930	14,500	20,760	20,100	17,700	16,340	19,720	27,450
Error (%)	0	1.5	-3.4	-5.3	-2.5	-5.6	-14.1	-1.8	12.6	-12.8	-0.5	-12.4	—	—	—	—
Q_{G+B}	30,880	26,300	33,970	33,980	28,720	41,010	36,650	39,660	31,010	24,830	33,640	32,710	28,810	25,430	32,890	38,390
$Q_{ALT/G+B}$	32,330	26,660	34,360	34,490	29,230	39,830	33,380	—	—	—	—	—	—	—	—	—
Error (%)	4.7	1.4	1.14	1.5	1.8	-2.8	-8.9	—	—	—	—	—	—	—	—	—

^aNote that for 2003 at Bahadurabad station, the monthly mean value of in situ discharge for November was not computed because of too numerous missing daily data and the mean climatological value for November was used to calculate the 2003 annual discharge.

of 15%–20%. In terms of annual averages (Table 4), as expected, the mean difference between altimetry-based and in situ discharge is low, with values reduced to less than 8% for the Ganga, less than 6% for the Brahmaputra and ~3% for the combined discharge G+B.

[56] For both stations, the year-to-year variations of peak flow are generally well captured, with low peak flows and high peak flows well depicted. The peak in $Q_{ALT/B}$ can be lower than the one observed in the in situ data (in 1995, 1996 and 1998 for instance), with nevertheless a maximum difference that never exceeds 15%. Note also that in 1998, 2007, and 2008, large peak discharges in the same order of magnitude are observed for the Brahmaputra River. Chowdhury [2003] and Mirza et al. [2003] reported that during the summer of 1998 over 60% of Bangladesh was inundated for nearly three months. Twice during 2007 the Brahmaputra flooded large areas of Bangladesh for periods between 1 and 2 weeks and in September 2008 more than half million people were affected by large floods in Northern Bangladesh.

[57] The total river discharge of the Ganga-Brahmaputra River system (Figure 12c), as expected, also shows a prominent seasonality with a maximum occurring usually in August, but with large year-to-year variations in the magnitude and, to some extent, in the timing of the peak. For 1993–2008 the annual maximum monthly discharge has a mean value of ~86,000 m³/s and a standard deviation ~14,400 m³/s. For 1993–2001, the comparison with in situ measurements (Q_{G+B}) shows an excellent agreement with underestimation of the discharge during the peak flow in some years of less than 10%. The largest yearly peak of $Q_{ALT/G+B}$, occurring in August and September 1998 with ~115,000 m³/s (~120,000 m³/s from in situ data) is associated with the simultaneous occurrence of discharge maxima in both rivers in late August and early September.

[58] To further evaluate the extended $Q_{ALT/G+B}$ (derived from ENVISAT only) for 2003–2008, when in situ discharge observations are no longer available, we compare the combined discharge $Q_{ALT/G+B}$ with GPCP precipitation estimates in the region that we spatially averaged over the Ganga and Brahmaputra catchments, upstream of the two gauging stations. Along with precipitation, we also considered another ENVISAT-derived river height estimated after the confluence of the two rivers (Figure 3). The ENVISAT virtual station is located at (23.42°N; 90.34°E). Note that this virtual station would have represented an excellent candidate to retrieve the G+B river discharge from altimetry. However, no in situ discharge measurements are available close to this point to construct the rating curve and no T-P data are available in this area.

[59] Figure 13 compares $Q_{ALT/G+B}$ with the two variables (normalized anomalies). In order to smooth out the high frequency variations (we are interested here in a qualitative assessment of the seasonal and interannual variations of our estimate), a moving average of ±1 month is applied to all the curves. There is an excellent agreement in the seasonal and interannual variations of the three time series for 2003–2008. The linear correlations between $Q_{ALT/G+B}$ and the two other variables are highly significant: 0.96 with the precipitation at one month lag and 0.89 with the ENVISAT-based river height ($p < 0.01$ above a correlation of 0.30 with 72 points). Moreover, all variables show a good agreement during the smaller peak flows observed in 2006 as well as

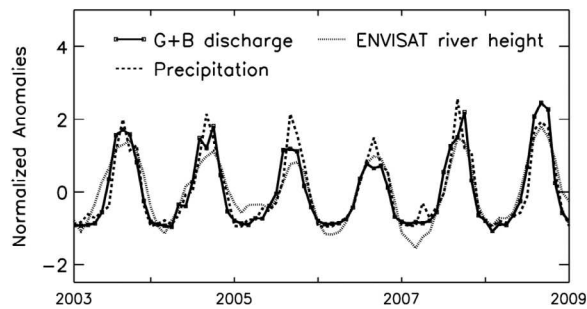


Figure 13. Time series of satellite-derived Ganga-Brahmaputra (G+B) river discharge (black solid line), precipitation estimates from GPCP (dashed line) and ENVISAT-derived river height (dotted line; the virtual station located at 23.42°N , 90.34°E is shown in Figure 3) during 2003–2008. All variables are normalized (the mean is subtracted and the resulting values are divided by the standard deviation over the period).

the larger peaks in 2007 and 2008. Especially, for 2006, the lowest peak discharge of 2003–2008, is associated with lowest summer precipitation over the same period and the 2008 large peak in the river discharge is associated with the largest positive anomaly observed in the 2008 precipitation. These comparisons give confidence in the altimetry-based total river discharge estimated for the Ganga and the Brahmaputra during 2003–2008.

5. Ganga-Brahmaputra Monthly Discharge Estimates at River Mouth for Oceanographic Applications

[60] For numerous studies related to the nearby ocean, the key factor is the continental discharge into the oceans. Hardinge and Bahadurabad, even if they represent a fair estimate of the total discharge of the two rivers, are still located tens of kilometers upstream of the river mouth.

[61] Usually, when time-varying river discharge information is not available, continent-to-ocean freshwater flux is estimated from climatologies. For the discharge of the Ganga-Brahmaputra into the Bay of Bengal, past studies have overcome this issue [Durand et al., 2007; Vinayachandran and Kurian, 2007] by using the runoff climatology from Vörösmarty et al. [1996] or Fekete et al. [2000]. These river discharge estimates at the river mouth, integrated over the entire Ganga and Brahmaputra watersheds, come from a combination of a climate-driven water balance model and, when available, observed river discharge information. In their simulations for the Ganga and Brahmaputra, Fekete et al. [2000] use in situ discharge at Bahadurabad (for 1969–1992) and at Farakka (1949–1974), also located on the Ganga River, ~ 80 km upstream of Hardinge (Figure 1b). Despite the different periods of observation and location, the mean monthly climatologies of the in situ discharge data sets used by Fekete et al. [2000] were found to be similar to the mean monthly climatologies of Q_G and Q_B estimated for 1993–2001.

[62] We propose a pragmatic way to adjust the altimetry-derived G+B flow to represent the river mouth outflow. The climatology from Fekete et al. [2000] (red curve) is shown in Figure 14a along with our climatology of $Q_{\text{ALT}/\text{G+B}}$ for

1993–2008 (black curve). The latter presents a climatological discharge slightly lower than the estimate of Fekete et al. [2000], especially from May to August. The difference between $Q_{\text{ALT}/\text{G+B}}$ and Fekete et al. [2000] is due to the fact that the latter integrates over the entire watersheds (Figure 1) and accounts for the contribution of local tributaries and precipitation downstream of Hardinge and Bahadurabad and after the Ganga and Brahmaputra confluence. In particular, their estimates include the discharge of the Meghna River (merging with the Ganga and Brahmaputra at 23.25°N). Some (limited) in situ observations of the Meghna discharge suggest that it yields about 10% of $Q_{\text{G+B}}$ at maximum.

[63] As a way of adjusting our data set to represent the flow at the river mouth, we scale it by a constant coefficient to constraint the long-term mean discharge to be identical to that of Fekete et al. [2000]. The ratio between the two estimates gives a coefficient of 118%, which we apply to $Q_{\text{ALT}/\text{G+B}}$ to get the so-called “ $Q_{\text{ALT}/\text{G+B}}$ scaled.” Figure 14a (green curve) shows the results. Though our result has the same long-term average as of Fekete et al. [2000] estimate, it exhibits slight differences in the seasonal evolution, with in particular a timing of the monsoonal increase different by about one month. In order to evaluate this scaling coefficient of 118%, we also estimated (1) the mean GPCP precipitation for 1993–2008 over the entire Ganga and Brahmaputra watersheds up to the river mouths and (2) the mean GPCP precipitation for 1993–2008 over the Ganga and Brahmaputra watersheds upstream of Hardinge and Bahadurabad, respectively. The ratio between

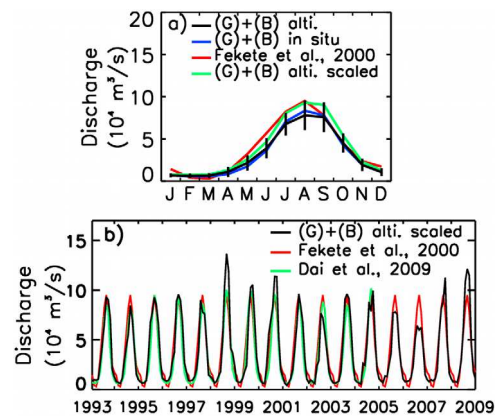


Figure 14. (a) The black line is the monthly climatology of the sum of the two discharges (G) and (B) derived from radar altimetry (1993–2008); the vertical bars show the monthly evolution of its interannual variability, defined by plus or minus one standard deviation; the blue line is the monthly climatology of the sum of the two discharges (G) and (B) derived from in situ measurements (1993–2001); the red line is the monthly climatology of the Ganga and Brahmaputra rivers discharge at the river mouth estimated by Fekete et al. [2000]; the green line is the same as the black line, after scaling by 118% (see the text for details). (b) 1993–2008 evolution of the satellite-derived Ganga-Brahmaputra River discharge (black line) at the river mouth (i.e., scaled), superimposed on the repeated climatology of Fekete et al. [2000] (red). The Ganga-Brahmaputra monthly river discharge at the river mouth from Dai et al. [2009] is shown in green for 1993–2004.

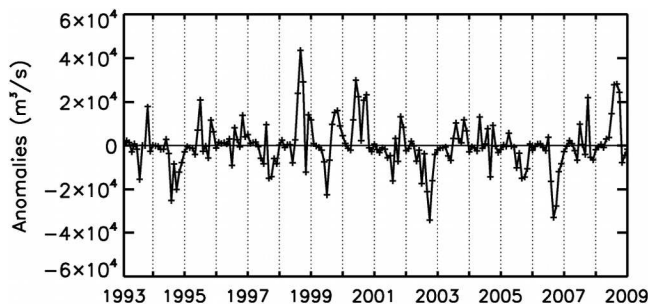


Figure 15. Deseasonalized anomalies (obtained by subtracting the 16 year mean monthly value from individual months) of the Ganga-Brahmaputra monthly river discharge at the river mouth for 1993–2008.

the two quantities is found to be 121%, a value on the same order of magnitude as the ratio between the mean discharge of *Fekete et al.* [2000] and the mean value of $Q_{ALT/G+B}$. Despite this good agreement, the scaling method we propose here has some limitations. For instance, such an approach does not take into account the influence of floodplains or irrigation networks downstream of Hardinge and Bahadurabad and their year-to-year variations that may exert on the discharge into the ocean. This should be investigated in future studies in a more comprehensive approach using evapotranspiration, floodplains extent, and water storage observations along with hydrological simulation [*Decharme et al.*, 2008].

[64] The coefficient of 118% is applied to $Q_{ALT/G+B}$ interannual monthly time series and the result is displayed in Figure 14b. In order to highlight the interannual variability of “ $Q_{ALT/G+B}$ scaled,” the repeated climatology from *Fekete et al.* [2000] is also shown. The standard deviation of their difference is $\sim 12,500 \text{ m}^3/\text{s}$, showing that the upscaled discharge presents a marked interannual variability much larger than the data set uncertainty. This value is really close to the one ($12,340 \text{ m}^3/\text{s}$) found in D10 when the same up-scaling adjustment in order was performed using in situ G+B discharges (Q_{G+B}) during 1992–1999 to force an ocean circulation model. Figure 14b also shows a comparison between “ $Q_{ALT/G+B}$ scaled” and the Ganga-Brahmaputra River discharge estimate from *Dai et al.* [2009]. Over 1993–2004, the standard deviation of their difference is $\sim 10,300 \text{ m}^3/\text{s}$ and the mean of their difference is about 13%. Over the period 1993–1995, both data sets agree well and the discharge values for the annual peak are almost identical. In contrast, for the period 1996–2004 the agreement between the two data sets is poorer. In particular, there is a large discrepancy during summer 1998, when the peak value in “ $Q_{ALT/G+B}$ scaled” is about 35% larger than the one from *Dai et al.* [2009]. Large differences are also observed in 2000 and 2002. As already seen in D10, these differences can be explained by the fact that, after 1996, Ganga river discharge estimates from *Dai et al.* [2009] are not based on observations but are constructed discharges based on CLM3 simulations. The moderate correlation of 0.7 for the Ganga between the CLM3 simulations and observed data during 1948–2004 [*Dai et al.*, 2009, see their Table 1] illustrates the difficulties of CLM3 to reproduce large anomalous events such as the one occurring in 1998.

[65] To reveal the nonseasonal variability of the Ganga-Brahmaputra monthly river discharge at the river mouth more clearly, we removed the 1993–2008 mean annual cycle to produce the deseasonalized anomalies shown in Figure 15. Pronounced oscillations about the mean with large interannual variations are clear. The peak-to-peak variability of interannual anomalies during one given year can be as large as $50,000 \text{ m}^3/\text{s}$. The two smallest anomalies in the record, $\sim -35,000 \text{ m}^3/\text{s}$ are observed in September 2002 and August 2006. The largest anomaly occurs in August 1998 with a discharge anomaly of $\sim 45,000 \text{ m}^3/\text{s}$. Other years with positive anomalies are 1999, 2000, and 2008. In 1999, though, large positive anomalies are seen only during August–December. Interestingly, one can see in Figure 15, that there are two periods during 1993–2008 where interannual anomalies of the same sign occur for a few consecutive years. For 1998–2000, the river discharge shows three consecutive years of relative strong positive anomaly whereas for 2005–2006, the river discharge shows two consecutive years of negative anomaly. These periods will be of particular interest for further studies regarding the impact of the Ganga-Brahmaputra River discharge on the Bay of Bengal, as they might favor the buildup of negative and positive anomalies in the sea surface salinity, possibly impacting the ocean temperature and thus the climate of the area.

6. Conclusion

[66] The aim of the present study was to produce a comprehensive monthly mean altimetry-derived Ganga-Brahmaputra River discharge data set for 1993–2008 for community use. We have examined more than a decade of daily in situ river discharge data for the Ganga and the Brahmaputra Rivers estimated at the points where they enter Bangladesh along with altimetry-derived river heights from multiple satellite missions, including TOPEX-Poseidon, ERS-2, and ENVISAT.

[67] We first compare nine direct measurements of Ganga in situ river heights made infrequently at Hardinge station during 2007 with altimeter-derived water levels from ENVISAT. The comparison for these nine points, representing a fair sample of the variability through a year with the water level varying $\sim 8 \text{ m}$ between the low and high water stages, shows good agreement between the two data sets with a correlation of 0.96 and a standard error of 0.26 m, which is in the typical range of accuracy of altimeter measurements over large rivers.

[68] Using in situ discharges and altimeter-derived water levels, we establish rating curves for both rivers using T-P and ERS-2 satellites. These rating curves are used to retrieve G and B discharges at 10 day (for 1993–2001) and 35 day (for 1995–2008) temporal sampling over the 16 year time span of T-P/ERS-2/ENVISAT altimetry. For the period 2003–2008, ENVISAT-derived discharges are estimated using the rating curves constructed with ERS-2 during 1995–2002, assuming that these rating curve equations remain valid for 2003–2008.

[69] The comparison of in situ and satellite-derived discharge estimates shows that the satellites reproduce the seasonal timing of the various stages of the hydrological regime (seasonal low/high water flow) as well as the interannual variations. For both rivers, T-P shows good results with low residuals (mean error on daily measurements about $\sim 15\%$ for

the Brahmaputra and ~30% for the Ganga). ERS-2-derived daily discharges are less accurate (mean error on daily measurements about ~29% for the Brahmaputra and ~36% for the Ganga) and a little above the acceptable accuracy (15%–20%) for discharge measurements. We evaluated the methodologies in various ways to confirm that the altimetry-based rating curves can be used with confidence to retrieve river discharge for periods when in situ data are not available or to extend the time series forwards. For instance, over the Brahmaputra, we showed that using ERS-2-based rating curve and ENVISAT measurements, the mean error on daily discharge estimates for 2003–2004 is ~22%. For most of the cases, the largest relative errors in the retrieved discharge are for the low flow period, and we showed that overall, for all the satellites, the errors are generally greatly reduced (below 20%, with for instance a mean error of 5.5% for T-P over the Brahmaputra) when only the high discharge season is considered. Around the yearly peak flow, we confirmed that the largest absolute errors are expected to occur when the sampling dates (10 or 35 days) bracket the peak flow date, with nevertheless, an underestimation or overestimation of the true mean discharge never exceeding 20%, still within the range of uncertainties acceptable for river discharge estimations. Regarding the error budget on daily discharge estimates over these two rivers, it will be interesting for future studies to investigate the separation of the individual contributing errors due to the instrument, the width of the river, the distance to the gauge or the temporal resolution.

[70] We then computed the Ganga, Brahmaputra and their aggregated discharges for 1993–2008 on a monthly basis. For each estimate, the seasonal and the year-to-year variations are captured and the low peak flows and high peak flows over the years are well depicted. The maximum difference with in situ data never exceeds 15%, showing that the errors of the estimated discharge using altimeter data are well within the range of acceptable errors (the standard deviation of the residuals is ~2700 m³/s). In terms of annual averages, the mean difference between altimetry-based and in situ discharge is less than 8% for the Ganga, less than 6% for the Brahmaputra and ~3% for the combined discharge G+B. For 2004–2008, when in situ data are no longer available, we assess the variability of the estimates against precipitation and river height after the confluence of the two rivers, showing good correspondence of interannual variations.

[71] Finally, because for studies related to the nearby ocean, the key factor is the continental discharge into the oceans, we presented a basic approach to infer Ganga-Brahmaputra altimetry-derived monthly discharge at the river mouths using an up-scaling approach against the climatology from *Fekete et al.* [2000]. The upscaled discharge exhibits a marked interannual variability with standard deviation in excess of ~12,500 m³/s, much larger than the data set uncertainty. Potential users of our product could easily do a similar analysis in order to scale our total Ganga-Brahmaputra discharge with respect to the climatology used in their own investigations.

[72] This new altimetry-derived discharge data set represents an unprecedented source of information to quantify freshwater flux in Indian Ocean circulation models. Indeed, together with the Argo project and SMOS satellite, which both provide routine salinity observations, our new estimates

will help to understand the impact of river discharge on the Bay of Bengal salinity and ultimately the climate variability of the region. Our estimates of Ganga-Brahmaputra River discharge will soon be extended to 2009 as ENVISAT is still delivering quality observations. Moreover, we will also use the new measurements from Jason-2, which was launched on June 2008, and provides observations over continental water bodies with the same 10 day sampling as T-P.

[73] As for the limitations of the approach discussed in this study, it is important to note here that it is still limited to rivers that are several kilometers wide because of the current satellite altimeters spatial resolution. Moreover, because of their orbit track separation at the equator (few tens to hundreds of kilometers), the spatial coverage of current satellite altimetry missions is not adequate for global scale investigations. These problems will be overcome in the future with a new generation of radar altimeters dedicated to continental hydrology, such as SWOT (Surface Water and Ocean Topography), as rivers with width on the order of 100 m and at global scale will be monitored with an averaging repeat cycle of 11 days. Improvements in altimeter spatial resolution will be also possible with the future altimetry mission such as SARAL/AltiKa (Ka band), which is planned to be launched in 2011 on the same orbit as ERS-2/ENVISAT.

[74] As already said, the monthly interval sampling we adopted in this study for our discharge data set corresponds both to the common time resolution of state-of-the-art discharge products [*Dai et al.*, 2009], and to the typical time scales satisfactorily resolved by actual ocean circulation models. With the progress of sensors and methods, it will be timely to extend our approach towards higher temporal frequencies. From the in situ river discharge data set, one can see indeed that there is significant energy in the discharge spectrum at intramonthly time scales. However, it will also take some time for ocean models to improve their skills at sub-monthly time scales in order to make the most of high-frequency (weekly or daily) discharge forcing fluxes.

[75] Finally, the methodology used in this study relies on the availability of some discharge ground-based measurements to determine the rating curves between altimetry-derived river water height and river discharge. As in situ observations are not always available to the scientific community, this prevents the use of this technique over other river basins where in situ measurements are not available. In preparation for SWOT, other promising approaches to derive river discharge from space, and which are not dependent on the availability of ground-based observations [*LeFavour and Alsdorf*, 2005] should be tested over the Ganga-Brahmaputra River system.

[76] **Acknowledgments.** We thank both anonymous reviewers who helped us to improve our manuscript. This study is funded by NASA's NEWS grant NNDX7AO90E managed by Jared K. Entin. We are indebted to the people who collected in situ hydrological observations. We thank Jean-Francois Crétaux (LEGOS-CNRS) for his suggestions and comments.

References

- Adler, R. F., et al. (2003), The Version 2 Global Precipitation Climatology Project (GPCP) monthly precipitation analysis 1979-present, *J. Hydro-meteorol.*, 4(6), 1147–1167.

- Alsdorf, D. E., and D. P. Lettenmaier (2003), Tracking fresh water from space, *Science*, 301(12), 1492–1494.
- Alsdorf, D. E., E. Rodríguez, and D. P. Lettenmaier (2007), Measuring surface water from space, *Rev. Geophys.*, 45, RG2002, doi:10.1029/2006RG000197.
- Berry, P. A. M. (2000), Topography from land radar altimeter data: Possibilities and restrictions, *Phys. Chem. Earth, Part A*, 25(1), 81–88, doi:10.1016/S1464-1895(00)00014-4.
- Berry, P. A. M., A. Jasper, and H. Bracke (1997), Retracking ERS-1 altimeter waveforms over land for topographic height determination: An expert system approach, *ESA Spec. Publ., ESA SP-414*, 403–408.
- Berry, P. A. M., J. D. Garlick, and E. L. Mathers (2004), Global scale monitoring of land surface water using multi-mission satellite radar altimetry, EGU 1st General Assembly, Nice, France.
- Berry, P. A. M., J. D. Garlick, J. A. Freeman, and E. L. Mathers (2005), Global inland water monitoring from multi-mission altimetry, *Geophys. Res. Lett.*, 32, L16401, doi:10.1029/2005GL022814.
- Birkett, C. M. (1998), Contribution of the TOPEX NASA radar altimeter to the global monitoring of large rivers and wetlands, *Water Resour. Res.*, 34(5), 1223–1239, doi:10.1029/98WR00124.
- Birkett, C. M., L. A. K. Mertes, T. Dunne, M. H. Costa, and M. J. Jasinski (2002), Surface water dynamics in the Amazon Basin: Application of satellite radar altimetry, *J. Geophys. Res.*, 107(D20), 8059, doi:10.1029/2001JD000609.
- Bjerklie, D. M., S. D. Lawrence, C. J. Vorosmarty, C. H. Bolster, and R. G. Congalton (2003), Evaluating the potential for measuring river discharge from space, *J. Hydrol.*, 278(1–4), 17–38, doi:10.1016/S0022-1694(03)00129-X.
- Callède, J., P. Kosuth, and E. De Oliveira (2001), Establishment of the stage–discharge relationship of the River Amazon at Óbidos: “Normal difference in level” method using “variable geometry,” *Hydrol. Sci. J.*, 46(3), 451–463.
- Calmant, S., F. Seyler, and J. F. Crétaux (2008), Monitoring continental surface waters by satellite altimetry, *Surv. Geophys.*, 29(4–5), 247–269, doi:10.1007/s10712-008-9051-1.
- Cazenave, A., P. C. D. Milly, H. Douville, J. Benveniste, P. Kosuth, and D. P. Lettenmaier (2004), Space techniques used to measure change in terrestrial waters, *Eos Trans. AGU*, 85(6), doi:10.1029/2004EO060006.
- Chowdhury, M. R. (2003), The El Niño–Southern Oscillation (ENSO) and seasonal flooding–Bangladesh, *Theor. Appl. Climatol.*, 76(1–2), 105–124.
- Chowdhury, M. R., and Y. Sato (1996), Flood monitoring in Bangladesh: Experience from normal and catastrophic floods, *J. Jpn. Assoc. Hydrol. Sci.*, 26, 241–252.
- Chowdhury, M. R., and N. Ward (2004), Hydro-meteorological variability in the Greater Ganges–Brahmaputra–Meghna Basins, *Int. J. Climatol.*, 24, 1495–1508, doi:10.1002/joc.1076.
- Coe, M. T., and C. M. Birkett (2004), Calculation of river discharge and prediction of lake height from satellite radar altimetry: Example for the Lake Chad basin, *Water Resour. Res.*, 40, W10205, doi:10.1029/2003WR002543.
- Crétaux, J. F., and C. Birkett (2006), Lake studies from satellite altimetry, *C. R. Geosci.*, 338(14–15), 1098–1112, doi:10.1016/j.crte.2006.08.002.
- Crétaux, J. F., A. V. Kouraev, F. Papa, M. Bergé-Nguyen, A. Cazenave, N. Aladin, and I. S. Plotnikov (2005), Evolution of sea level of the big Aral Sea from satellite altimetry and its implications for water balance, *J. Great Lakes Res.*, 31, 520–534.
- Crétaux, J. F., S. Calmant, R. Abarca del Rio, A. Kouraev, and M. Bergé-Nguyen (2010), Lake studies from satellite altimetry, in *Coastal Altimetry*, edited by S. Vignudelli et al., Springer, Berlin.
- Dai, A., and K. E. Trenberth (2002), Estimates of freshwater discharge from continents: Latitudinal and seasonal variations, *J. Hydrometeorol.*, 3(6), 660–687.
- Dai, A., T. Qian, and K. E. Trenberth (2009), Changes in continental freshwater discharge from 1948 to 2004, *J. Clim.*, 22(10), 2773–2792, doi:10.1175/2008JCLI2592.1.
- Decharme, B., H. Douville, C. Prigent, F. Papa, and F. Aires (2008), A new river flooding scheme for global climate applications: Off-line validation over South America, *J. Geophys. Res.*, 113, D11110, doi:10.1029/2007JD009376.
- Durand, F., D. Shankar, C. de Boyer Montégut, S. S. C. Shenoi, B. Blanke, and G. Madec (2007), Modeling the barrier-layer formation in the south-eastern Arabian Sea, *J. Clim.*, 20(10), 2109–2120, doi:10.1175/JCLI4112.1.
- Fekete, B. M., C. J. Vörösmarty, and W. Grabs (2000), Global, composite runoff fields based on observed river discharge and simulated water balances. Documentation for UNH-GRDC Composite Runoff Fields, v.1.0, Global Runoff Data Center, Koblenz, Germany.
- Frappart, F., S. Calmant, M. Cauhopé, F. Seyler, and A. Cazenave (2006), Validation of ENVISAT RA-2 derived water levels over the Amazon basin, *Remote Sens. Environ.*, 100, 252–264.
- Frappart, F., F. Papa, J. S. Famiglietti, C. Prigent, W. B. Rossow, and F. Seyler (2008), Interannual variations of river water storage from a multiple satellite approach: A case study for the Rio Negro River basin, *J. Geophys. Res.*, 113, D21104, doi:10.1029/2007JD009438.
- Fu, L. L., and A. Cazenave (2001), *Satellite altimetry and Earth sciences, A Handbook of techniques and applications. International Geophysics Series*, 69, Academic, San Diego.
- Global Runoff Data Centre (2009), Long-Term Mean Monthly Discharges and Annual Characteristics of GRDC Station/Global Runoff Data Centre, Koblenz, Federal Institute of Hydrology (BfG).
- Hoyos, C. D., and P. J. Webster (2007), The role of intraseasonal variability in the nature of Asian monsoon precipitation, *J. Clim.*, 20, 4402–4424.
- Jian, J., P. J. Webster, and C. D. Hoyos (2009), Large-scale controls on Ganges and Brahmaputra river discharge on intraseasonal and seasonal time scales, *Q. J. R. Meteorol. Soc.*, 135, 353–370, doi:10.1002/qj.384.
- Kerr, Y. H., P. Waldteufel, J.-P. Wigneron, J.-M. Martinuzzi, J. Font, and M. Berger (2001), Soil moisture retrieval from space: The soil moisture and ocean salinity (SMOS) mission, *IEEE Trans. Geosci. Remote Sens.*, 39, 1729–1735.
- Kouraev, A. V., E. A. Zakharova, O. Samain, N. M. Mognard, and A. Cazenave (2004), Ob River discharge from Topex-Poseidon satellite altimetry (1992–2002), *Remote Sens. Environ.*, 93, 238–245.
- LeFavour, G., and D. Alsdorf (2005), Water slope and discharge in the Amazon River estimated using the shuttle radar topography mission digital elevation model, *Geophys. Res. Lett.*, 32, L17404, doi:10.1029/2005GL023836.
- Leon, J. G., S. Calmant, F. Seyler, M. P. Bonnet, M. Cauhopé, and F. Frappart (2006), Rating curves and average water depth at the Upper Negro river from satellite altimetry and modelled discharges, *J. Hydrol.*, 328(3–4), 481–496.
- McPhaden, M. J., G. R. Foltz, T. Lee, V. S. N. Murty, M. Ravichandran, G. A. Vecchi, J. Vialard, J. D. Wiggert, and L. Yu (2009), Ocean-atmosphere interactions during cyclone nargis, *Eos Trans. AGU*, 90(7), 53–60, doi:10.1029/2009EO070001.
- Mirza, M. M. (2003), The choice of stage–discharge relationship for the Ganges and Brahmaputra rivers in Bangladesh, *Nord. Hydrol.*, 34(4), 321–342.
- Mirza, M. M. Q., R. A. Warrick, and N. J. Erickson (2003), The implications of climate change on floods of the Ganges, Brahmaputra and Meghna rivers in Bangladesh, *Clim. Change*, 57(3), 287–318.
- Papa, F., C. Prigent, F. Durand, and W. B. Rossow (2006), Wetland dynamics using a suite of satellite observations: A case study of application and evaluation for the Indian Subcontinent, *Geophys. Res. Lett.*, 33, L08401, doi:10.1029/2006GL025767.
- Papa, F., C. Prigent, and W. B. Rossow (2008a), Monitoring flood and discharge variations in the large Siberian rivers from a multi-satellite technique, *Surv. Geophys.*, 29(4–5), 297–317, doi:10.1007/s10712-008-9036-0.
- Papa, F., A. Güntner, F. Frappart, C. Prigent, and W. B. Rossow (2008b), Variations of surface water extent and water storage in large river basins: A comparison of different global data sources, *Geophys. Res. Lett.*, 35, L11401, doi:10.1029/2008GL033857.
- Papa, F., C. Prigent, F. Aires, C. Jimenez, W. B. Rossow, and E. Matthews (2010), Interannual variability of surface water extent at global scale, 1993–2004, *J. Geophys. Res.*, 115, D12111, doi:10.1029/2009JD012674.
- Rahman, S. H., D. Sengupta, and M. Ravichandran (2009), Variability of Indian summer monsoon rainfall in daily data from gauge and satellite, *J. Geophys. Res.*, 114, D17113, doi:10.1029/2008JD011694.
- Rantz, S. E., et al. (1982), Measurement and computation of streamflow: Volume 2. Computation of discharge, *Water Supply Paper 2175, U.S. Geol. Surv.*, pp. 285–631.
- Rémy, F., and S. Parouty (2010), Antarctic Ice Sheet and Radar Altimetry: A Review, *Remote Sens.*, 1, 1212–1239, doi:10.3390/rs1041212.
- Schott, F. A., S.-P. Xie, and J. P. McCreary Jr. (2009), Indian Ocean circulation and climate variability, *Rev. Geophys.*, 47, RG1002, doi:10.1029/2007RG000245.
- Sengupta, D., G. N. Bharath Raj, and S. S. C. Shenoi (2006), Surface freshwater from Bay of Bengal runoff and Indonesian Throughflow in the tropical Indian Ocean, *Geophys. Res. Lett.*, 33, L22609, doi:10.1029/2006GL027573.
- Sengupta, D., B. R. Goddalahundi, and D. S. Anitha (2008), Cyclone-induced mixing does not cool SST in the post-monsoon North Bay of Bengal, *Atmos. Sci. Lett.*, 9(1), 1–6, doi:10.1002/asl.162.
- Shenoi, S. S. C., D. Shankar, and S. R. Shetye (2002), Differences in heat budgets of the near-surface Arabian Sea and Bay of Bengal: Implications

- for the summer monsoon, *J. Geophys. Res.*, 107(C6), 3052, doi:10.1029/2000JC000679.
- Shetye, S. R. (1993), The movement and implications of the Ganges-Brahmaputra run off on entering the Bay of Bengal, *Curr. Sci.*, 64(1), 32–38.
- Vinayachandran, P. N., and J. Kurian (2007), Hydrographic observations and model simulation of the Bay of Bengal freshwater plume, *Deep Sea Res., Part I*, 54, 471–486.
- Vinayachandran, P. N., and R. S. Nanjundiah (2009), Indian Ocean sea surface salinity variations in a coupled model, *Clim. Dyn.*, 33, 245–263, doi:10.1007/s00382-008-0511-6.
- Vinayachandran, P. N., V. S. N. Murty, and V. Ramesh Babu (2002), Observations of barrier layer formation in the Bay of Bengal during summer monsoon, *J. Geophys. Res.*, 107(C12), 8018, doi:10.1029/2001JC000831.
- Vörösmarty, C. J., B. Fekete, and B. A. Tucker (1996), River discharge database, Version 1.0 (RivDIS v1.0), Volumes 0 through 6. A contribution to IHP-V Theme: 1. Technical documents in hydrology series, Tech. Rep., UNESCO, Paris.
- Xie, P., and P. Arkin (1997), Analyses of global monthly precipitation using gauge observations, satellite estimates, and numerical model predictions, *J. Clim.*, 9, 840–858.
- Zakharova, E. A., A. V. Kouraev, A. Cazenave, and F. Seyler (2006), Amazon River discharge estimated from TOPEX/Poseidon altimetry, *C. R. Geosci.*, 338, 188–196.
-
- S. K. Bala, Institute of Water and Flood Management, Bangladesh University of Engineering and Technology, Dhaka 1000, Bangladesh.
- F. Durand, IRD–LEGOS, BP A5, F-98848 Nouméa CEDEX, New Caledonia.
- F. Papa, IRD–LEGOS, 14 Ave. Edouard Belin, F-31400 Toulouse, France. (fpapa@giss.nasa.gov)
- A. Rahman and W. B. Rossow, NOAA–CREST, City College of New York, Steinman Hall, T-107, 140th St. and Convent Ave., New York, NY 10031, USA.